

Theoretical insights into the nature of synergistic enhancement in bimetallic CoTiAlPO-5 catalysts for ammonia activation

M. E. Potter,^{a*} K. McColl,^b F. Corà,^b A. B. Levy^c and R. Raja^a

Received 00th January 20xx,
Accepted 00th January 20xx

DOI: 10.1039/x0xx00000x

www.rsc.org/

Bimetallic catalytic synergy, the concurrent action of two different metal ions in the same material, has resulted in improved efficiency in many catalytic systems and for a range of chemical processes. Via a computational mechanistic study, we investigate the catalytic benefits of the bimetallic CoTiAlPO-5 material in comparison to the monometallic CoAlPO-5 system, on the activation of NH₃. The presence of Ti in a framework site adjacent to Co stabilises the Co(II) oxidation state, and increases the Co(III)/Co(II) reduction potential. We show that this change lowers the activation barrier for the homolytic H extraction from NH₃ by Co(III), from 162 kJ/mol in the monometallic CoAlPO-5 catalyst to 140 kJ/mol in the bimetallic CoTiAlPO-5 (175 and 111 kJ/mol respectively when considering both dispersion and free energy corrections). Elucidation of mechanistic details through computational studies can make significant contributions to the rational design of catalytic materials.

Introduction

The development of novel catalytic systems is fundamental in the pursuit of sustainable chemical processes. To maximise catalytic efficacy, a range of factors and structure-property correlations must be conscientiously modulated, through rigorous and adroit synthetic protocols.¹⁻⁹ The rational design of novel bimetallic heterogeneous catalysts has received significant attention; recent successes, including nanoparticles,³ mixed metal oxides⁴ and metal dopants,⁵ demonstrate that the intrinsic behaviour of an active metal centre can be attuned by a second metal site.¹⁻⁹ However the second metal site garners further levels of complexity, introducing new metal-framework and metal-metal interactions. Yet, knowledge of these interactions is necessary towards intelligent and rational catalytic design.^{1,8}

Numerous examples show the catalytic advantages of bimetallic substitution in aluminophosphate (AIPO) frameworks. AIPOs consist of alternating Al(III) and P(V) oxidic corner-sharing tetrahedra, forming structures akin to zeolites. A range of different dopants can be introduced into the frameworks, based on oxidation state and ionic radius, allowing many metallic substituent pairings for different chemical processes.¹⁰⁻¹⁴ Recently we performed a combined experimental and computational (X-ray Adsorption Spectroscopy and periodic Density Functional Theory) study to probe the nature of the synergistic enhancement within the CoTiAlPO-5 catalyst (where both cobalt and titanium ions are isomorphously substituted into the same AIPO-5 framework).^{13,14} The improved catalytic activity has been attributed to the close proximity of the cobalt

and titanium dopants. The metal pairing was initially found to make the Ti(IV) ions increasingly tetrahedral, compared to monometallic TiAlPO-5. This is notable as a tetrahedral geometry has been found to aid oxidant activation in other titanium-containing materials including TS-1 and Ti-MCM-41.^{15,16} This study also demonstrated that a significant proportion of the cobalt and titanium atoms are in adjacent framework sites, forming a distorted Co-O-Ti bridge. The presence of the adjacent titanium was found to modify the III/II redox energy of the framework cobalt ions, from -1.2 to -1.7 eV using H₂ as reductant (Figure 1), accounting for improvements in oxidation catalysis.^{13,14,17-19}

Theoretical studies play a significant role in understanding monometallic active sites in zeotype catalysts.²⁰⁻²⁴ Primarily these studies focus on the properties and characteristics of metal species,²⁰⁻²² with more recent studies probing the mechanistic pathways, for example of hydrocarbon activation.²³⁻²⁵ Scarce few studies have addressed the features of bimetallic species.^{2,25} In this work we employ electronic structure calculations to investigate the likely initial stages of the activation of ammonia, and contrast the behaviour of cobalt in monometallic CoAlPO-5 and in the bimetallic CoTiAlPO-5.

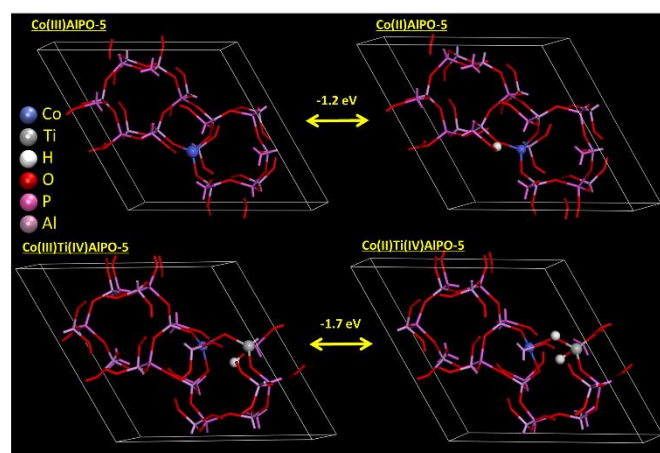


Figure 1. Illustration of the titanium ability to attune the redox properties of CoAlPO-5. Redox potentials are calculated as the energy change in: $\text{Co(III)AlPO-5} + \frac{1}{2}\text{H}_2 \rightarrow \text{H-Co(II)AlPO-5}$ as per reference 17.

^a Department of Chemistry, University of Southampton, Department of Chemistry, University Road, Southampton, Hants, SO17 1BJ, UK.

^b Department of Chemistry, University College London, 20 Gordon Street, London, WC1H 0AJ, UK.

^c Honeywell Int, 101 Columbia Road, Morristown, NJ 07962, USA.

*M.E.Potter@soton.ac.uk

Electronic Supplementary Information (ESI) available: This includes geometric information on monometallic and bimetallic systems. Coordination geometries of ammonia-bound species, energy profile of non-catalytic ammonia activation, Γ -point phonon modes for the transition states, further figures on the evolution of bond lengths and spin for the radical formation and radical stabilization steps. See DOI: 10.1039/x0xx00000x

On obtaining a deeper appreciation of the mechanistic processes it is believed that the results yielded here will aid the future rational design of catalytic systems. In situ production of NH_2OH from NH_3 is critical for processes of industrial relevance, such as the ammoximation of cyclohexanone to ϵ -caprolactam, an important precursor for the production of nylon-6.¹⁸

Experimental section

Periodic Density Functional Theory (DFT) electronic structure calculations were performed on the University of Southampton Iridis3 and the UK national HPC service Archer, using the same setup discussed in detail in reference 14. We used the CRYSTAL code²⁶ and the B3LYP hybrid-exchange functional.^{27–30} The AFI framework was calculated using periodic boundary conditions in P1 space group to allow full-optimisation without symmetry constraints. The electronic distribution was described as a linear combination of atomic orbitals and the basis functions are expressed as Gaussian-type orbitals. Aluminium, phosphorus, oxygen and hydrogen ions were described using a double valence plus polarization basis set whereas titanium and cobalt were described using a triple-valence plus polarization basis set. All basis sets employed were taken from the online library for the CRYSTAL code.³¹ The AFI structure was described by modelling one unit cell containing 72 atoms (12 AlPO_4 formula units).¹⁴ Cobalt was substituted for aluminium and titanium was substituted for phosphorus. In the case of a charge imbalance (Co(II) substituting Al(III) or Ti(IV) substituting for P(V)) a proton was attached to an oxygen ion adjacent to the divalent or tetravalent dopant. One substitution was made per metal per unit cell, corresponding to 8.3 mol% loading.¹⁴ In all cases the high-spin configuration was found to be the ground electronic state. The initial geometries were taken from our previous work, where all possible positions of charge balancing protons and adjacent titanium atom were calculated with the unit cell parameters left unconstrained.¹⁴ The lowest energy combinations were selected and used in this work. In this work the unit cell parameters were kept constant for calculating the energy of the system. Transition state geometries were obtained by calculating the internal energy of the system along the relevant reaction coordinates through constrained geometry optimizations where the reaction coordinate was fixed and all other degrees of freedom allowed to relax. The reaction coordinate has been varied in steps of 0.1 Å or less, between its value in reagent and products. Transition state geometries, identified as the local internal energy maximum along the reaction coordinate, have been refined via second derivative methods and eigenvector-following modes. In all cases we found the initial constrained calculations reproduce the correct transition state to within 0.1 kJ/mol in energy and 0.01 Å in geometry.

Internal energies have been corrected for an estimate of dispersion through the empirical scheme proposed by Grimme.³² Vibrational contributions (zero point energy and vibrational entropy) have also been added to reagents, products and transition states to estimate the reaction free energies at room temperature.

Results and discussions

Internal energies

In this section we report and discuss results concerning the internal energies calculated at B3LYP level. Dispersion and free energy corrections from vibrational modes are considered in section 2.

The activation of ammonia to form hydroxylamine (NH_2OH) occurs through aerobic oxidation of ammonia with molecular oxygen.^{18,19} For the first step in our mechanistic study we have therefore investigated the binding of these reagents on the monometallic catalysts: Ti(IV)AlPO-5 and Co(II/III)AlPO-5, whose geometric structures are summarized in Tables S1–S5, further details in reference 14. Neither metal showed significant interaction with molecular oxygen (less than 13 kJ/mol, Table 1), and both oxygen atoms reside at least 3.0 Å away from the metal center in all cases. The slight energetic stabilization observed is in the region expected for Van der Waals interactions between a molecule and a pore wall (Table 1, Tables S6–S8).³³

In contrast all metal ions interact with ammonia (Table 1 and Tables S9–S11), through the Lewis acid/base interaction between the lone pair of electrons on the nitrogen and the electron-deficient metal centre; adsorption on the metal is favoured over interaction with the Brønsted acid protons. This was confirmed by using a range of initial geometries of ammonia within the unit cell, all of which eventually converged on a M– NH_3 bond regardless of whether ammonia was placed near a Brønsted acid site for all systems.

This behavior is analogous to that of ethane in MnAlPO-5.^{23,24} The binding energy increases with the metal oxidation state, as the metal becomes increasingly electron deficient and molecule. Interaction between ammonia and the bimetallic Co(III)Ti(IV)AlPO-5 showed ammonia preferentially bound to cobalt, not titanium (Table 2, Tables S12 and S13), in contrast to

Table 1 Binding energies and metal-N/O distance of ammonia and oxygen with specific metal centres in the monometallic catalysts.

System	M– NH_3		M– O_2	
	Binding energy/(kJ mol ^{−1}) ^a	M–N distance/Å	Binding energy/(kJ mol ^{−1})	M–O distance/Å
Co(II)AlPO-5	−56.1	2.22	−4.7	3.22
Co(III)AlPO-5	−63.4	2.21	−6.0	3.42
Ti(IV)AlPO-5	−107.9	2.25	−12.3	3.00

Table 2 NH_3 binding energies and metal–N distance in Co(III)Ti(IV)AlPO-5.

Atom bound to NH_3	Binding energy/(kJ mol ^{−1}) ^a	M–N distance/Å
Co(III)	−82.2	2.19
Ti(IV)	−32.8	2.23

a) Binding energy was calculated thus:

$$E_{\text{binding}} = E[\text{M}^{n+}\text{AlPO-5} + \text{Probe}] - E[\text{M}^{n+}\text{AlPO-5}] - E[\text{Probe}]$$

therefore a better acceptor for the σ -donating ammonia the trend observed for the monometallic systems (Table 1). While the adsorption energy of ammonia on Co(III) increases from -63.4 kJ mol⁻¹ in the monometallic catalyst to -82.2 in the bimetallic, the adsorption energy for Ti decreases from -107.9 to -32.8, despite showing similar M-NH₃ bond distances to the monometallic species. This is therefore primarily due to the local environment around Co and Ti before and after the binding process. Before interacting with NH₃ Co(III) adopts a distorted tetrahedral environment, with one bond (1.93 Å) clearly longer than the other three (1.86, 1.76 and 1.74 Å). On binding to the NH₃ a trigonal bipyramidal environment evolves around the cobalt center (Figure S1), where the longer bond extends, naturally adopting the axial position trans to NH₃. In contrast the Ti(IV) environment is made of two short bonds (1.74 and 1.77 Å) and two longer bonds (1.93 and 1.98 Å). Our previous work showed that these two longer bonds are due to the distortion associated with the Co-O-Ti bridge (1.93 Å) and the protonated oxygen in the Ti-OH-Al species (1.98 Å). Therefore to accommodate the ammonia, the already distorted Co-O-Ti and Ti-OH-Al bonds would have to distort further still, extending the bond lengths and weakening the interactions. This would result in a less energetically favourable system. The bimetallic cobalt site, in comparison, only has one distorted bond to accommodate, hence why Ti is not the preferred site for ammonia adsorption in the bimetallic system. We also demonstrated that the electron density of protonated oxygen atoms is lower than other framework oxygen atoms,¹⁴ which leads to a weaker bond with the metal site. On binding to ammonia the Ti(IV) site also adopts a trigonal bipyramidal coordination, however the protonated oxygen is forced to become axial, further weakening the Ti-OH bond and making the coordination far less favorable. Given the minimal change in spin of the framework oxygens and the cobalt on binding to ammonia it is believed that the geometric effects are the main reason behind the difference in binding energies in the monometallic and bimetallic systems.

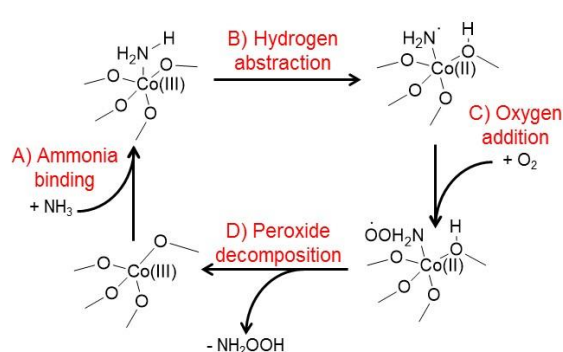
To become 'active' cobalt-containing APOs must be calcined so cobalt reaches the trivalent oxidation state required to initiate oxidation reactions.³⁵ The role that Ti(IV) substituted APOs play

in oxidation catalysis is still unclear; however, all our calculations on reduced bimetallic CoTiAlPO-5 systems always converge to Co(II) and Ti(IV) and do not converge on Co(III) and Ti(III) oxidation states. It is therefore reasonable to assume that Co is the redox active metal site responsible for NH₃ activation. As such we now dedicate the rest of this script to contrasting the role of the cobalt sites in the monometallic CoAlPO-5 and bimetallic CoTiAlPO-5 species. No interaction was observed between ammonia and oxygen either in the pore, or between individual gaseous ammonia and oxygen atoms. These factors coupled with the binding energies

(Table 1) show that the initial step of this reaction involves an interaction between ammonia and a Co(III) active site. This is in agreement with previous findings on ethane oxidation catalysed by MnAlPO-5, which shows that the rate-determining step is the initial activation of the organic substrate to form a radical species.^{23,24} Activation of ethane by MnAlPO-5, calculated with the same settings as in the present work, requires an activation energy of 135 kJ/mol, with a reaction enthalpy of 93 kJ/mol.^{23,24}

We suggest a similar mechanism for the activation of ammonia (Scheme 1), comprising the elementary steps of adsorption, hydrogen abstraction and O₂ addition resulting in the production of NH₂OO· radicals.^{36,37} We hypothesise that this intermediate follows a peroxide decomposition pathway into hydroxylamine, likely via NH₂OOH (however this is not known experimentally).³⁸⁻⁴⁰ In this paper we focus on the initial stages of ammonia activation, the hydrogen abstraction and O₂ addition steps, in order to gain an improved insight into the behavior of the mono- and bi-metallic CoTiAlPO-5 catalyst for oxidation catalysis.

Similarly to the preactivation step of alkane oxidation,²³⁻²⁵ the radical formation step occurs via homolytic cleavage of one N-H bond on a Co(III) site, to form an amide radical (Scheme 1B) and a reduced Co(II) site. The energy profile of this reaction step is examined by performing a series of constrained geometry optimizations, in which a reaction coordinate (in this case the O_{Framework} - H_{Ammonia} distance) is progressively varied from its value in the reagents (ammonia adsorbed on Co(III)) to that in the products.



Scheme 1 Proposed reaction mechanism for the activation of ammonia showing 4 key steps: A) Ammonia binding, B) Hydrogen abstraction, C) Oxygen addition and D) Peroxide decomposition.

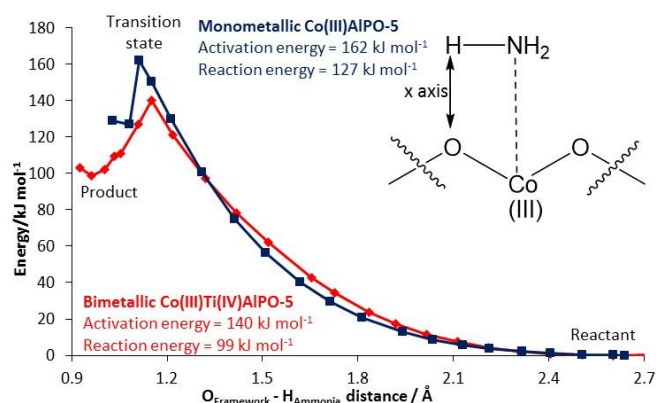


Figure 2 Internal energy profile for the ammonia activation step in monometallic Co(III)AlPO-5 and bimetallic Co(III)Ti(IV)AlPO-5.

As the O-H distance contracts, the N-H bond weakens, producing the amide radical and simultaneously reducing the cobalt ion. Of the four oxygens adjacent to the cobalt ion, the *specific* oxygen to be protonated was chosen as the one which resulted in the lowest energy proton position in the corresponding Co(II) system.¹⁴ In the monometallic species the reaction corresponds to $\text{Co}^{\text{III}}(\text{OP})_4$ becoming $\text{Co}^{\text{II}}(\text{OP})_3(\text{OHP})$; in the bimetallic catalyst the proton binds to the oxygen of the Co-O-Ti bridge to give a Co-OH-Ti species species, i.e. from $\text{Co}^{\text{III}}(\text{OP})_3(\text{OTi})$ to $\text{Co}^{\text{II}}(\text{OP})_3(\text{OHTi})$ (Tables S1-S4 and S7-S10).

The energy profiles for the radical formation step in monometallic and bimetallic systems are shown in Figure 2. The full set of Γ -point phonon modes calculated for all transition states (Figures S12-S15) discussed here are reported in the SI, to show they have the correct structure with only one imaginary mode. In both monometallic and bimetallic systems the reaction is highly endothermic, with the transition state close to the product in both activation energy and reaction coordinate. Breaking the N-H bond in the absence of a catalyst was calculated to require 470 kJ/mol (Figure S3), explaining the endothermic nature of the process and the need for a catalyst. Both the activation and reaction energies are lower in bimetallic Co(III)Ti(IV)AlPO-5 than in the monometallic Co(III)AlPO-5 (Figure 2), while the transition state for the bimetallic system occurs at a longer O-H distance, in accordance with the lower activation energy. The O-H distance of the product is significantly shorter in the bimetallic system than in the monometallic. This is attributed to a different coordination of the amide radical to the Co(II) site, as discussed below. The energy values calculated here are higher but comparable to those calculated for the activation of ethane with MnAlPO-5, of 135 and 93 kJ/mol.^{23,24} This is a result of the different bond dissociation energies for ammonia and ethane (470 and 410 kJ/mol respectively), thus cleavage of the stronger N-H bond requires higher activation and reaction energies.⁴¹

Analysis of atomic distances and spin densities provides further mechanistic insights. The initial electron spin of cobalt ($3.04 |e|$) is consistent with Co(III) (Table S4; Figures S4 and S5), and is constant up to the transition state. While tetrahedral high-spin Co(III) is expected to have 4 unpaired electrons, it is noted that the system is not perfectly tetrahedral and spin-leaching occurs onto the neighbouring oxygen atoms. On reaching the transition state (O-H distance 1.11 \AA monometallic, 1.15 \AA bimetallic) the cobalt spin is lowered to roughly $2.7 |e|$, consistent with an homolytic mechanism and the reduction of Co(III) to Co(II) (Figures S4 and S5).¹⁴ We have already discussed in ref. 14 that the redox potential of Co(III) is influenced by the presence of adjacent titanium ions.¹⁴ Reduction of cobalt from Co(III) to Co(II) alleviates the build-up of electron spin of the specific (protonated) framework oxygen in the bimetallic CoTiAlPO-5 system more than in the monometallic. In the ammonia activation reaction step the oxygen spin evolution follows similar behaviour.

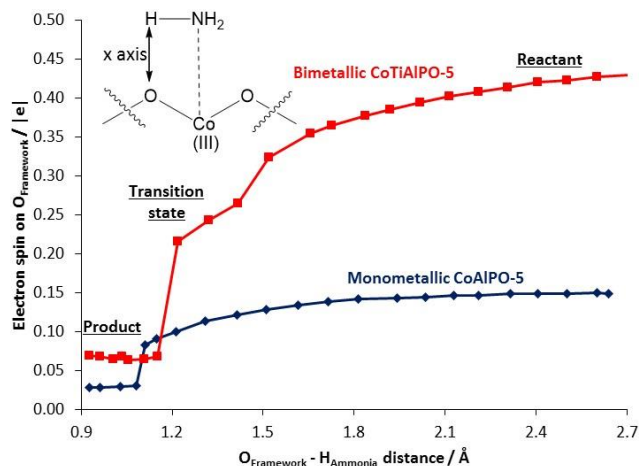


Figure 3 Comparison of the spin evolution on the framework oxygen in the monometallic and bimetallic systems.

The spin polarization of the specific framework oxygen in the bimetallic system is reduced from $0.43 |e|$ to $0.07 |e|$ (Figure 3) on protonation, whereas the spin polarization of the same specific framework oxygen in the monometallic CoAlPO-5 system reduces from $0.15 |e|$ to $0.03 |e|$ (Figure 3). The greater alleviation of spin on the oxygen makes this step less endothermic for the bimetallic system than the monometallic. We also suggest that the greater spin polarization on the bridging oxygen makes it more active for the activation of homolytic bond dissociations.

Comparing changes in the N-H and Co-N distances of the two systems reveals fundamental differences. In the monometallic CoAlPO-5 system (Figure S6) the amide radical, once formed, moves away from the cobalt ion (the Co-N distance elongates from 2.21 \AA to 3.22 \AA , Figure S6), but retains an interaction with the hydrogen atom abstracted, resulting in a shorter N-H distance (1.72 \AA). The cobalt adopts a distorted tetrahedral geometry. Interaction with the amide radical results in a particularly long equilibrium O-H distance of 1.08 \AA . In contrast, for the bimetallic CoTiAlPO-5 system, the Co-N distance remains roughly constant throughout the reaction step (from 2.19 \AA to 2.00 \AA , Figure S7), and an elongation of the N-H distance occurs (from 1.02 \AA to 2.66 \AA , Figure S7). The O-H distance is not affected by interaction with the amide radical, and is measured as 0.96 \AA . Co retains the trigonal bipyramidal geometry. This behaviour is due to the enhanced stability and bond strength of the framework oxygen-proton bond in the bimetallic system.¹⁴ The stronger interaction between the framework oxygen and the proton weakens the proton-amide interaction, and in turn promotes the Co-amide interaction. By retaining a strong interaction with the amide radical, the cobalt in the bimetallic system contributes to delocalize the spin of the molecule; the spin density of the nitrogen atom is of $0.92 |e|$ in the bimetallic system, compared to $1.07 |e|$ in the monometallic system (Figures S4 and S5).

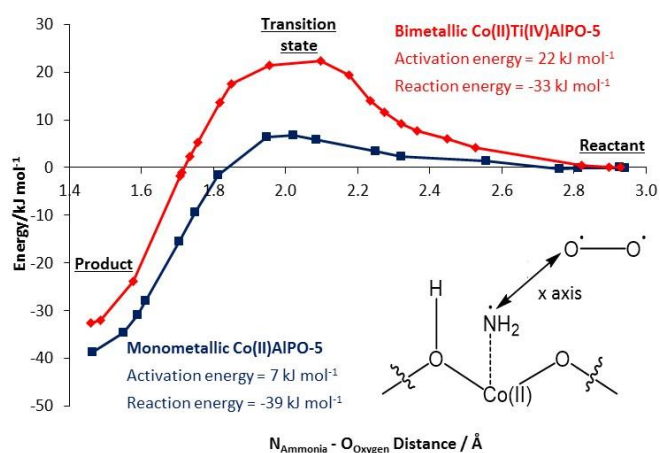


Figure 4 Contrasting the energy profile of NH_2OO formation for monometallic Co(II)AlPO-5 and bimetallic $\text{Co(II)Ti(IV)AlPO-5}$.

These findings suggest that the lower reaction and activation energies for the bimetallic CoTiAlPO-5 system, in this reaction step, are due to increased stability of the Co(II) , and the increased spin stabilization of the bimetallic framework oxygen and the amide intermediate.¹⁴

Once generated, the amide radical intermediate is stabilised by addition of triplet oxygen (Scheme 1C, Figure 4), as was the case for alkyl radicals in hydrocarbon oxidation reactions.^{23,24} Calculations of the energy profile as a function of the $\text{N}_{\text{Ammonia}} - \text{O}_{\text{oxygen}}$ distance (Scheme 1C) shows that addition of oxygen is exothermic and requires a significantly lower activation energy than the radical formation step in both systems. Both activation and reaction energy of the oxygen addition step are lower for CoAlPO-5 than CoTiAlPO-5 (Figures 2 and 4). This is attributed to the Co-N interaction discussed earlier. While in the monometallic system the amide is only loosely bound to Co (the Co-N equilibrium bond distance is of 3.28 \AA , Figure S6 and S8), it is strongly adsorbed in the bimetallic system (2.00 \AA , Figure S7 and S9). The Co-N distance is constant in the radical stabilisation step for the monometallic system, as the bond is already broken (Figure S8).

In the bimetallic system the Co-N distance extends as the $\text{NH}_2\text{OO}\cdot$ radical forms, as required to break the Co-N bond (expanding from 2.00 to 2.83 \AA , Figure S9) accounting for the increased activation and reaction energies of the bimetallic system. The calculated energy profiles are different to those for the analogous radical stabilisation step for ethane and MnAlPO-5 , which show no activation barrier and are heavily stabilized by -149 kJ/mol .^{23,24} In contrast the monometallic and bimetallic systems calculated here show an activation barrier of 7 and 22 kJ/mol respectively, and are stabilized to a lesser extent of -39 and -33 kJ/mol respectively. The difference is due to the weaker N-O bond formed here relative to the C-O bond in the ethane oxidation.^{42,43} Comparison of the mechanisms shows that the monometallic system behaves in an analogous way to the MnAlPO-5 system. Both break the metal-radical bond (Co-N and Mn-C) in the radical formation step, as the radical maintains an interaction with the abstracted proton.

The electron spins of the two systems (Figure S10 and S11), provide some mechanistic insight.

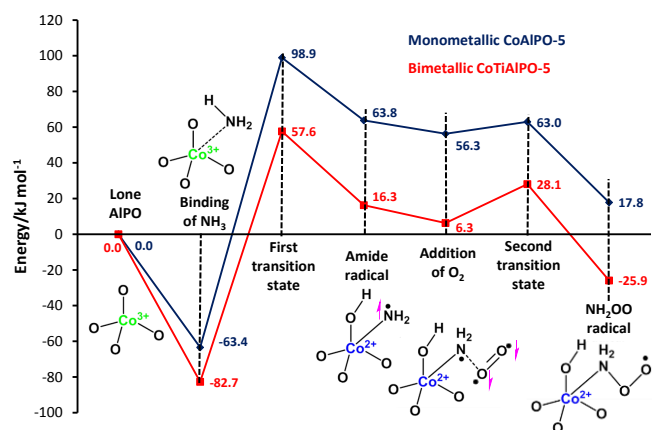


Figure 5 Complete energetic profile of the two reaction steps examined, in mono and bimetallic catalysts.

As oxygen approaches the amide radical, a covalent bond forms involving the α electron of the amide and a β electron on the oxygen (O1). This is seen by the short N-O bond length of the product (1.46 \AA for both monometallic and bimetallic) and also by the total spin decreasing by roughly $2|e|$ in both systems. Only very slight differences were observed in the cobalt and nitrogen spins between the two systems (Figures S10 and S11), despite the difference in bond lengths. This suggests that the strength of the amide stabilisation by complexation of Co(II) is the primary factor in the energy difference between mono- and bi-metallic catalysts in the radical stabilisation step.

The energetic profile of the two steps discussed here is shown in Figure 5. The rate determining step is the hydrogen abstraction from NH_3 , leading the radical formation, in accordance with previous work.^{14,23,24} The lower activation energy calculated for this step in the bimetallic system over the monometallic provides mechanistic detail concerning the benefits of bimetallic substitution.

Dispersion corrections and free energy

The energy values discussed in section 1 refer to internal energies from the original B3LYP DFT calculations. This functional does not account for dispersion forces, that we have estimated using the empirical D2 correction proposed by Grimme.³² We have also estimated the vibrational contribution to free energy (zero point energy and vibrational entropy) at room temperature for reagents, products and transition states using the geometries identified in section 1.

Results for the NH_3 activation and O_2 addition steps in both mono and bi-metallic catalysts are summarized in Table 3. While dispersion increases, as expected, the adsorption energies of NH_3 and O_2 molecules on the active sites, it has smaller effect on reaction and activation energies (Figure S16).

NH_3 activation comprises a H-transfer step with minor changes of bond distances other than those involving the N and H atoms of the bond being cleaved, while O_2 addition too requires

Table 3 Summary of calculated activation and reaction energies (kJ/mol) for NH₃ activation and O₂ addition steps in mono and bi-metallic catalysts, including dispersion and entropic contributions.

Monometallic reaction step		Reaction energies/(kJ mol ⁻¹)			
		Electronic energy	Electronic energy + dispersion	Free energy	Free energy + dispersion
Step A. Ammonia binding	$\Delta E_{\text{NH}_3}^{\text{ads}}$	-63.4	-100.8	-41.7	-77.7
Step B. Hydrogen abstraction	E_a^{B}	162.3	185.3	151.7	174.6
	ΔE^{B}	127.2	148.1	111.4	133.2
Step C. Oxygen addition	$\Delta E_{\text{O}_2}^{\text{ads}}$	-7.5	-26	6.7	-12.4
	E_a^{C}	6.7	12.6	10.2	15.9
	ΔE^{C}	-38.5	-43.9	-33.1	-32.2
Bimetallic reaction step		Reaction energies/(kJ mol ⁻¹)			
		Electronic energy	Electronic energy + dispersion	Free energy	Free energy + dispersion
Step A. Ammonia binding	$\Delta E_{\text{NH}_3}^{\text{ads}}$	-82.7	-97.2	-56.1	-70.6
Step B. Hydrogen abstraction	E_a^{B}	138.9	128.6	121.5	111.1
	ΔE^{B}	98.0	87.7	84.6	74.4
Step C. Oxygen addition	$\Delta E_{\text{O}_2}^{\text{ads}}$	-9.7	-28.9	7.1	-11.6
	E_a^{C}	21.6	20.9	20.7	20.1
	ΔE^{C}	-53.6	-46.0	-46.7	-39.1

relatively small atomic displacements (the N-based radical is oriented away from the framework) that cause small changes in dispersion. Dispersion however enhances the overall difference between the activation energy for NH₃ activation in mono and bimetallic catalysts, due to the different coordination geometry of the $\cdot\text{NH}_2$ radical in the two cases, as discussed in section 1. Vibrational contributions to the free energy also have relatively small effects (of less than 15 kJ/mol, Figure S17) on reaction and activation energies of both reaction steps. Despite O₂ addition causing a decrease in the number of molecules, because O₂ prior to the reaction is not rotationally and translationally free but confined in the AlPO-5 pores and weakly interacting with the framework (rotational and translational modes of O₂ correspond to frequencies ranging between 40 and 150 cm⁻¹), its loss in translational and rotational entropy is substantially smaller than in the equivalent gas-phase reaction. Despite the actual reaction and activation energies show some dependence on whether and how dispersion and entropic contributions are included (Figure S18), the overall picture of the reaction mechanism is unchanged, with the NH₃ activation being the rate determining step, and the bimetallic catalyst showing much enhanced activity over the monometallic for this reaction step.

Conclusions

By employing periodic DFT calculations we have shown the benefits of bimetallic substitution in microporous AlPO catalysts. Through careful investigation of the initial reaction steps of the aerobic activation of ammonia we have revealed that the activation energy of the rate determining radical formation step can be lowered through the application of a bimetallic CoTiAlPO-5 catalyst, enhancing catalytic activity over the monometallic CoAlPO-5 catalyst. Ti does not directly take part in the catalytic reaction, but its presence in a framework

site adjacent to Co modifies substantially the adsorption energy of ammonia, and the Co(III)/Co(II) reduction potential, stabilising the 2+ oxidation state and hence all those elementary reaction steps that occur through reduction of Co(III). These include the radical H abstraction from NH₃ that initiates (and is the limiting step for) the *in situ* production of hydroxylamine. The bridging framework oxygen between Co and Ti has a prominent role in the synergic enhancement of catalytic activity. Its location between one electron rich (Co(III), d⁶) and one electron poor (Ti(IV), d⁰) transition metal ion contributes to the delocalisation of the Co(III) spin density. In the bare CoTiAlPO-5 catalyst, the bridging oxygen has a noticeable spin polarisation of 0.419 |e| that activates its reactivity in elementary steps that require radical formation. We have shown that design strategies aimed at developing improved catalysts for ammonia activation should be targeted at minimizing the activation barrier for the radical formation step. The lower activation energy calculated for the bimetallic system over the monometallic shows the enhanced activity and provides an atomistic explanation for the bimetallic synergy observed experimentally.

Acknowledgements

MEP and RR gratefully acknowledge Honeywell LLC for funding. Archer access (<http://www.archer.ac.uk>) was granted through membership of the UK's HEC Materials Chemistry Consortium, funded by EPSRC (EP/L000202).

References

- 1 R. Raja, M. E. Potter and S. H. Newland, *Chem. Commun.*, 2014, **50**, 5940-5957.
- 2 R. D. Oldroyd, J. M. Thomas and G. Sankar, *Chem. Commun.*, 1997, **21**, 2025-2056.

- 3 L. Kesavan, R. Tiruvalam, M. H. Ab Rahim, M. I. bin Saiman, D. I.; Enache, R. L. Jenkins, N. Dimitratos, J. A. Lopez-Sanchez, S. H. Taylor, D. W. Knight, C. J. Kiely and G. J. Hutchings, *Science*, 2011, **331**, 195–199.
- 4 M. R. Morrill, N. T. Thao, H. Shou, R. J. Davis, D. G. Barton, D. Ferrari, P. K. Agrawal and C. W. Jones, *ACS Catal.*, 2013, **3**, 1665–1675.
- 5 D. Zhang, Y. Wei, L. Xu, F. Chang, Z. Liu, S. Meng, B. L. Su and Z. Liu, *Micropor. Mesopor. Mater.*, 2008, **116**, 684–692.
- 6 R. D. Adams, B. Captain, W. Fu, M. B. Hall, J. Manson, M. D. Smith and C. E. Webster, *J. Am. Chem. Soc.*, 2004, **126**, 5253–5267.
- 7 S. Fietcher, I. Dorbandt, P. Bogdanoff, G. Zehl, H. Schulenburg, H. Tributsch, M. Bron, J. Radnik and M. Fieber-Erdmann, *J. Phys. Chem. C*, 2007, **111**, 477–487.
- 8 D. M. Alonso, S. G. Wettstein and J. A. Dumesic, *Chem. Soc. Rev.*, 2012, **41**, 8075–8098.
- 9 P. Visuvamithiran, K. Shanthi, M. Palanichamy and V. Murugesan, *Catal. Sci. Technol.*, 2013, **3**, 2340–2348.
- 10 R. M. Leithall, V. N. Shetti, S. Maurelli, M. Chiesa, E. Gianotti and R. Raja, *J. Am. Chem. Soc.*, 2013, **135**, 2915–2918.
- 11 L. Zhou, J. U. H. Miao, X. Li and F. Wang, *Catal. Lett.*, 2005, **99**, 231–234.
- 12 E. Gianotti, M. Manzoli, M. E. Potter, V. N. Shetti, D. Sun, A. J. Paterson, T. M. Mezza, A. Levy and R. Raja, *Chem. Sci.*, 2014, **5**, 1810–1819.
- 13 J. Paterson, M. E. Potter, E. Gianotti and R. Raja, *Chem. Commun.*, 2011, **47**, 517–519.
- 14 M. E. Potter, A. J. Paterson, B. Mishra, S. D. Kelly, S. R. Bare, F. Cora', A. B. Levy and R. Raja, *J. Am. Chem. Soc.*, 2015, **137**, 8534–8540.
- 15 M. G. Clerici, G. Bellussi and U. Romano, *J. Catal.*, 1991, **129**, 159–167.
- 16 P. E. Sinclair, G. Sankar, C. R. A. Catlow, J. M. Thomas and T. Maschmeyer, *J. Phys. Chem. B*, 1997, **101**, 4232–4237.
- 17 I. Saadoun, F. Cora', M. Alfredsson and C. R. A. Catlow, *J. Phys. Chem. B*, 2003, **107**, 3012–3018.
- 18 R. Raja, *US Patent*, 2010, US2010/0179317 A1.
- 19 J. M. Thomas and R. Raja, *Proc. Natl. Acad. Sci. U. S. A.*, 2005, **102**, 13732–13736.
- 20 F. Cora', M. Alfredsson, C. M. Barker, R. G. Bell, M. D. Foster, I. Saadoun, A. Simplerer and C. R. A. Catlow, *J. Solid State Chem.*, 2003, **176**, 496–529.
- 21 C. M. Barker, D. Gleeson, N. Kaltsoyannis, C. R. A. Catlow, G. Sankar and J. M. Thomas, *Phys. Chem. Chem. Phys.*, 2002, **4**, 1228–1240.
- 22 E. L. Uzunova, H. Mikosch and J. Hafner, *J. Phys. Chem. C*, 2008, **112**, 2632–2639.
- 23 L. Gomez-Hortiguera, F. Cora', G. Sankar, C. M. Zicovich-Wilson and C. R. A. Catlow, *Chem. – Eur. J.*, 2010, **16**, 13638–13645.
- 24 L. Gomez-Hortiguera, F. Cora' and C. R. A. Catlow, *ACS. Catal.*, 2011, **1**, 18–28.
- 25 L. Gomez-Hortiguera, F. Cora' and C. R. A. Catlow, *Phys. Chem. Chem. Phys.*, 2013, **15**, 6870–6874.
- 26 R. Dovesi, R. Orlando, B. Civalleri, C. Roetti, V. R. Saunders and C. M. Zicovich-Wilson, *Z. Kristallogr.*, 2005, **220**, 571–573.
- 27 A. D. Becke, *J. Chem. Phys.*, 1993, **98**, 5648–5652.
- 28 C. Lee, W. Yang and R. G. Parr, *Phys. Rev. B*, 1988, **37**, 785–789.
- 29 S. H. Vosko, L. Willk and M. Nusair, *Can. J. Phys.*, 1980, **58**, 1200–1211.
- 30 P. J. Stephens, F. J. Devlin, C. F. Chabalowski and M. J. Frisch, *J. Phys. Chem.*, 1994, **98**, 11623–11627.
- 31 CRYSTAL Basis Sets Library.
(http://www.crystal.unito.it/Basis_Sets/Ptable.html)
accessed July 2016.
- 32 S. Grimme, *J. Comp. Chem.*, 2006, **27**, 1787–1799.
- 33 L. Gomez-Hortiguera, F. Cora', C. R. A. Catlow and J. Perez-Pariente, *J. Am. Chem. Soc.*, 2004, **126**, 12097–12102.
- 34 C. Glidewell, *J. Coord. Chem.*, 1977, **6**, 189–192.
- 35 P. A. Barrett, G. Sankar, C. R. A. Catlow and J. M. Thomas, *J. Phys. Chem.*, 1996, **100**, 8977–8985.
- 36 R. Sumathi and S. D. A. Peyerimhoff, *Chem. Phys. Lett.*, 1996, **263**, 742–748.
- 37 A. Samuni, S. Goldstein, A. Russo, J. B. Mithcell, M. C. Krishna and P. Neta, *J. Am. Chem. Soc.*, 2002, **124**, 8719–8724.
- 38 L. Gomez-Hortiguera, F. Cora' and C. R. A. Catlow, *ACS. Catal.*, 2011, **1**, 945–955.
- 39 L. Gomez-Hortiguera, F. Cora' and C. R. A. Catlow, *ACS Catal.*, 2011, **1**, 1487–1497.
- 40 L. Gomez-Hortiguera, F. Cora' and C. R. A. Catlow, *ACS Catal.*, 2011, **1**, 1475–1486.
- 41 B. S. Jursic, *J. Chem. Soc., Perkin Trans. 2*, 1999, **2**, 369–372.
- 42 G. Glockler, *J. Phys. Chem.*, 1958, **62**, 1049–1054.
- 43 G. Glockler, *J. Chem. Phys.*, 1951, **19**, 124–125.

SUPPLEMENTARY INFORMATION

Theoretical insights into the nature of synergistic enhancement in bimetallic CoTiAlPO-5 catalysts for ammonia activation

Matthew E. Potter,^{a,*} Kit McColl,^b Furio Corà,^b Alan B. Levy^c and Robert Raja^a

^a Department of Chemistry, University of Southampton, Department of Chemistry, University Road, Southampton, Hants, SO17 1BJ, UK.

^b Department of Chemistry, University College London, 20 Gordon Street, London, WC1H 0AJ, UK.

^c Honeywell Int, 101 Columbia Road, Morristown, NJ 07962, USA.

Contents

Calculated equilibrium geometries of mono- and bi-metallic catalysts	Page S2
Calculated equilibrium geometries of bound monometallic catalysts	Page S4
Calculated equilibrium geometries of bound bimetallic catalysts	Page S7
DFT calculated NH ₃ coordination geometries	Page S8
Non catalytic N-H activation energy profile	Page S9
Hydrogen abstraction step	Page S10
Evolution of spin	Page S10
Evolution of bond lengths	Page S11
Oxygen addition step	Page S12
Evolution of bond lengths	Page S12
Evolution of spin	Page S13
Transition state vibrational frequency calculations	Page S14
Monometallic hydrogen abstraction transition state	Page S14
Bimetallic hydrogen abstraction transition state	Page S15
Monometallic oxygen addition transition state	Page S16
Bimetallic oxygen addition transition state	Page S17
Transition state figures	Page S19
Complete energetics	Page S21
Electronic energy + dispersion	Page S21
Free energy	Page S21
Free energy + dispersion	Page S22

Calculated equilibrium geometries of mono- and bi-metallic catalysts

Monometallic Co(II)AlPO-5

Table S1: Bond lengths in monometallic Co(II)AlPO-5.

Atom 1	Atom 2	Bond length/Å
Co1	O1 (H1)	2.120
Co1	O2	1.871
Co1	O3	1.897
Co1	O4	1.876
O1 (H1)	P1 (H1)	1.608
O2	P2	1.518
O3	P3	1.520
O4	P4	1.524
O1	H1	0.992

Monometallic Co(III)AlPO-5

Table S2: Bond lengths in monometallic Co(III)AlPO-5.

Atom 1	Atom 2	Bond length/Å
Co1	O1	1.816
Co1	O2	1.820
Co1	O3	1.837
Co1	O4	1.822
O1	P1	1.548
O2	P2	1.545
O3	P3	1.541
O4	P4	1.546

Monometallic Ti(IV)AlPO-5

Table S3: Bond lengths in monometallic Ti(IV)AlPO-5.

Atom 1	Atom 2	Bond length/Å
Ti1	O1 (H1)	1.987
Ti1	O2	1.775
Ti1	O3	1.765
Ti1	O4	1.751
O1 (H1)	Al1 (H1)	1.792
O2	Al2	1.700
O3	Al3	1.711
O4	Al4	1.751
O1	H1	0.970

Bimetallic Co(II)Ti(IV)AlPO-5**Table S4:** Bond lengths in bimetallic Co(II)Ti(IV)AlPO-5.

Atom 1	Atom 2	Bond length/Å
Co1	O1 (H1) (Bridge)	1.973
Co1	O2	1.909
Co1	O3	1.782
Co1	O4	2.005
Ti1	O1 (H1) (Bridge)	1.961
Ti1	O5 (H2)	1.983
Ti1	O6	1.731
Ti1	O7	1.719
O2	P1	1.514
O3	P2	1.519
O4	P3	1.540
O5 (H2)	Al1 (H2)	1.801
O6	Al2	1.703
O7	Al3	1.731
O1 (H1) (Bridge)	H1	0.973
O5 (H2)	H2	0.982

Bimetallic Co(III)Ti(IV)AlPO-5**Table S5:** Bond lengths in bimetallic Co(III)Ti(IV)AlPO-5.

Atom 1	Atom 2	Bond length/Å
Co1	O1 (Bridge)	1.757
Co1	O2	1.860
Co1	O3	1.743
Co1	O4	1.931
Ti1	O1 (Bridge)	1.928
Ti1	O5 (H1)	1.988
Ti1	O6	1.744
Ti1	O7	1.768
O2	P1	1.534
O3	P2	1.534
O4	P3	1.557
O5 (H1)	Al1 (H1)	1.805
O6	Al2	1.665
O7	Al3	1.726
O5 (H1)	H1	0.975

Calculated equilibrium geometries of bound monometallic catalysts

Table S6: Bond lengths in monometallic Co(II)AlPO-5 bound to O₂.

Atom 1	Atom 2	Bond length/Å
Co1	O1 (H)	2.120
Co1	O2	1.881
Co1	O3	1.900
Co1	O4	1.876
O1 (H)	P1 (H)	1.608
O2	P2	1.517
O3	P3	1.519
O4	P4	1.518
O1 (H)	H1	0.992
Co1	O5	3.215
Co1	O6	4.135
O5	O6	1.227

Table S7: Bond lengths in monometallic Co(III)AlPO-5 bound to O₂.

Atom 1	Atom 2	Bond length/Å
Co1	O1	1.838
Co1	O2	1.826
Co1	O3	1.835
Co1	O4	1.819
O1	P1	1.541
O2	P2	1.548
O3	P3	1.540
O4	P4	1.545
Co1	O5	3.423
Co1	O6	4.097
O5	O6	1.227

Table S8: Bond lengths in monometallic Ti(IV)AlPO-5 bond to O₂.

Atom 1	Atom 2	Bond length/Å
Ti1	O1 (H)	1.995
Ti1	O2	1.760
Ti1	O3	1.768
Ti1	O4	1.751

O1 (H)	Al1 (H)	1.791
O2	Al2	1.701
O3	Al3	1.713
O4	Al4	1.711
O1 (H)	H1	0.696
Ti1	O5	3.001
Ti1	O6	3.746
O5	O5	1.227

Table S9: Bond lengths in monometallic Co(II)AlPO-5 bound to NH₃.

Atom 1	Atom 2	Bond length/Å
Co1	O1	1.814
Co1	O2	1.838
Co1	O3	1.852
Co1	O4	1.964
O1	P1	1.536
O2	P2	1.535
O3	P3	1.527
O4	P4	1.526
Co1	N1	2.208
N1	H1	1.017
N1	H2	1.017
N2	H3	1.019

Table S10: Bond lengths in monometallic Co(III)AlPO-5 bound to NH₃.

Atom 1	Atom 2	Bond length/Å
Co1	O1 (H)	2.136
Co1	O2	1.953
Co1	O3	1.981
Co1	O4	1.923
O1 (H)	P1 (H)	1.596
O2	P2	1.509
O3	P3	1.512
O4	P4	1.508
O1 (H)	H1	1.001
Co1	N1	2.215
N1	H2	1.017
N1	H3	1.018
N2	H4	1.018

Table S11: Bond lengths in monometallic Ti(IV)AlPO-5 bound to NH₃.

Atom 1	Atom 2	Bond length/Å
Ti1	O1 (H)	2.097
Ti1	O2	1.789
Ti1	O3	1.801
Ti1	O4	1.760
O1 (H)	Al1 (H)	1.759
O2	Al2	1.709
O3	Al3	1.690
O4	Al4	1.704
O1 (H)	H1	0.968
Ti1	N1	2.254
N1	H2	1.017
N1	H3	1.019
N2	H4	1.021

Calculated equilibrium geometries of bound bimetallic catalysts

Table S12: Bond lengths in bimetallic Co(III)Ti(IV)AlPO-5 with ammonia bound to the cobalt site.

Atom 1	Atom 2	Bond length/Å
Co1	O1 (Bridge)	1.733
Co1	O2	1.862
Co1	O3	1.887
Co1	O4	2.122
Ti1	O1 (Bridge)	1.745
Ti1	O5	1.747
Ti1	O6	1.806
Ti1	O7 (H1)	1.978
O2	P1	1.514
O3	P2	1.543
O4	P3	1.530
O5	Al1	1.726
O6	Al2	1.722
O7 (H1)	Al3	1.776
O7 (H1)	H1	0.969
Co1	N1	2.186
N1	H2	1.017
N1	H3	1.018
N1	H4	1.019

Table S13: Bond lengths in bimetallic Co(III)Ti(IV)AlPO-5 with ammonia bound to the titanium site.

Atom 1	Atom 2	Bond length/Å
Co1	O1 (Bridge)	1.726
Co1	O2	1.844
Co1	O3	1.871
Co1	O4	1.873
Ti1	O1	1.750
Ti1	O5	1.761
Ti1	O6	1.844
Ti1	O7 (H1)	2.008
O2	P1	1.514
O3	P2	1.543
O4	P3	1.530
O5	Al1	1.729
O6	Al2	1.722
O7 (H1)	Al3	1.776
O7 (H1)	H1	0.969
Ti1	N1	2.239
N1	H2	1.019
N1	H3	1.020
N1	H4	1.021

DFT Calculated NH₃ coordination geometries

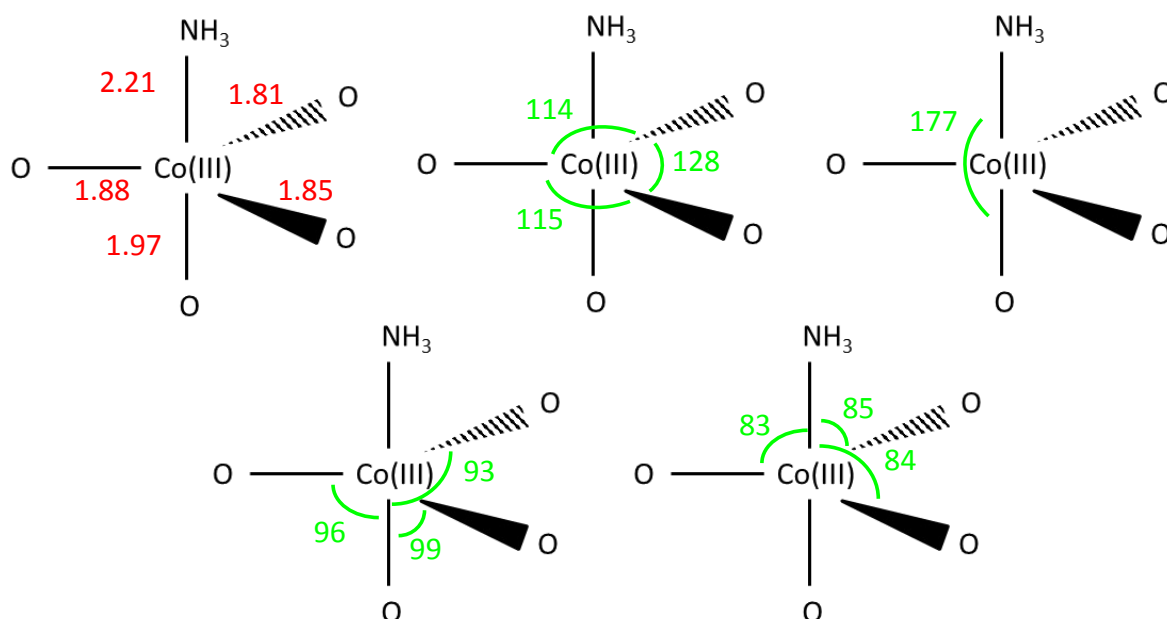


Figure S1: Geometric coordination of NH₃ to monometallic Co(III)AlPO-5 showing the trigonal bipyramidal shape. Red numbers represent lengths in angstroms, green values are angles in degrees.

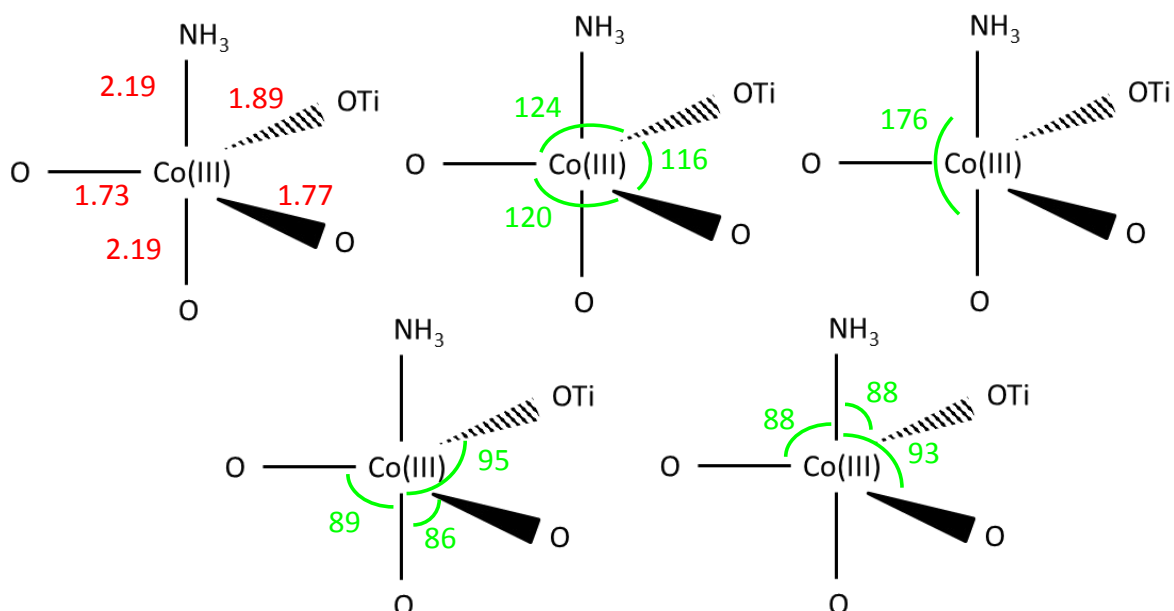


Figure S2: Geometric coordination of NH₃ to bimetallic Co(III)Ti(IV)AlPO-5 showing the trigonal bipyramidal shape. Red numbers represent lengths in angstroms, green values are angles in degrees.

Non-catalytic N-H activation energy profile

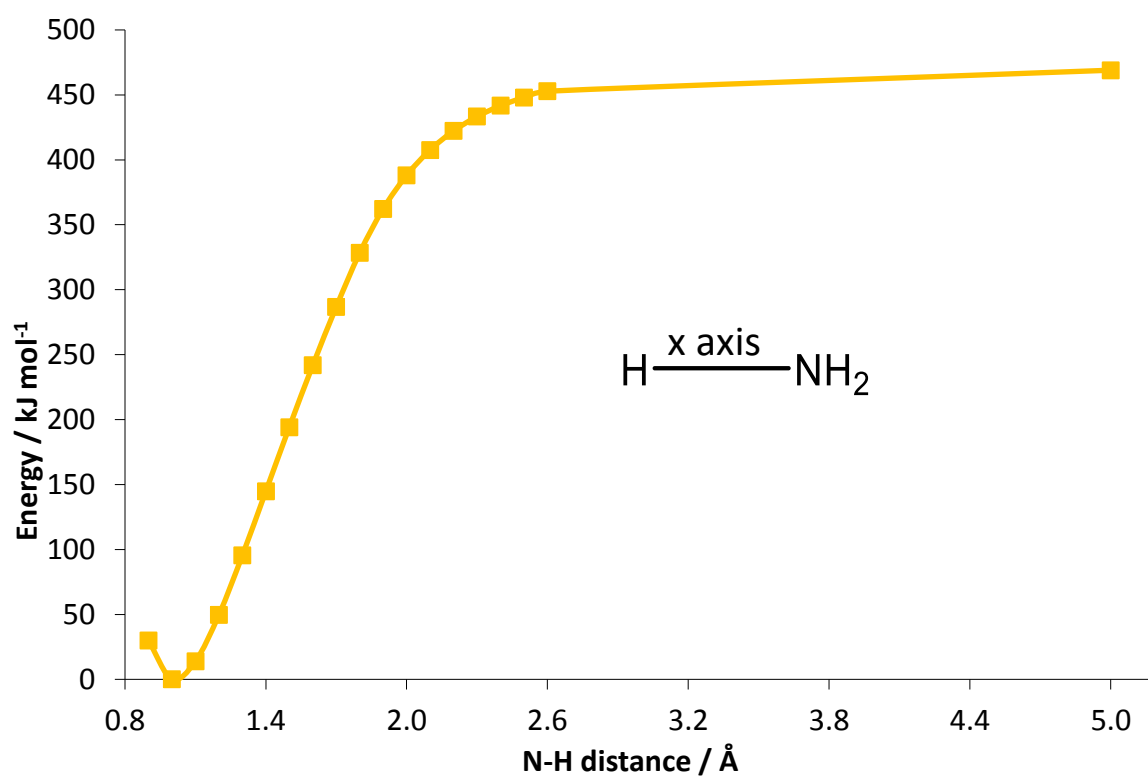


Figure S3: Energy profile showing that 470 kJ/mol is required to break the H—NH₂ bond non-catalytically.

Hydrogen abstraction step

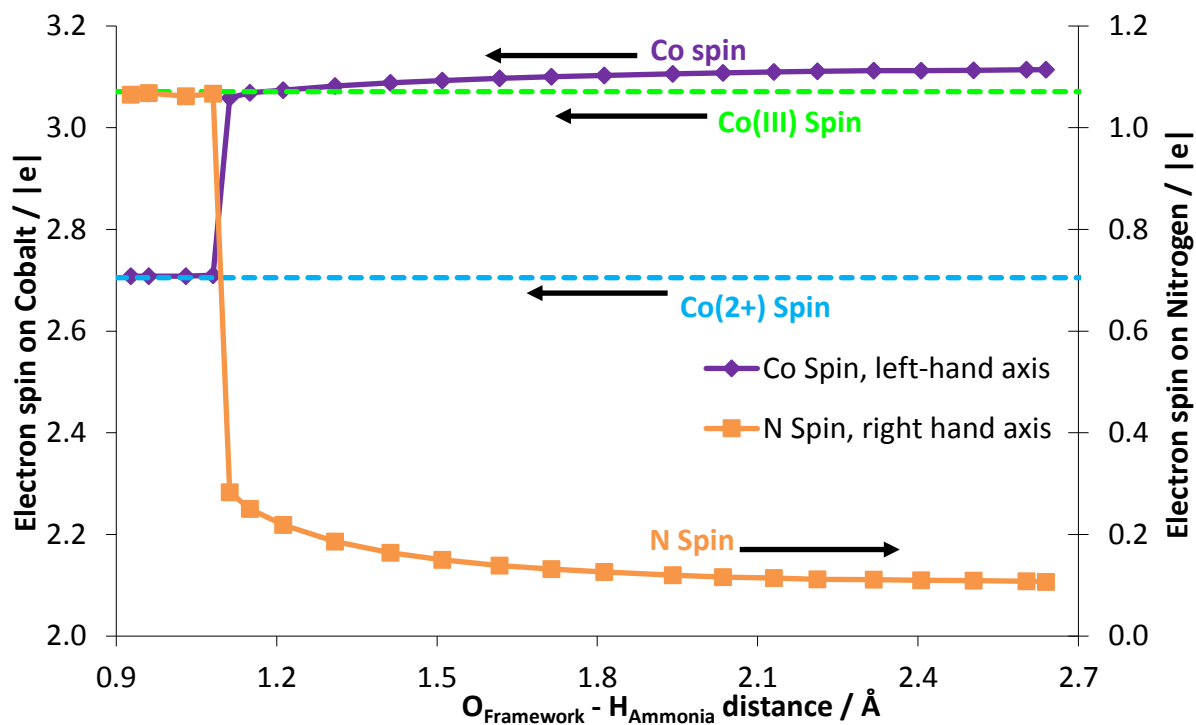


Figure S4: Spin evolution of monometallic CoAlPO-5 for the activation of ammonia.

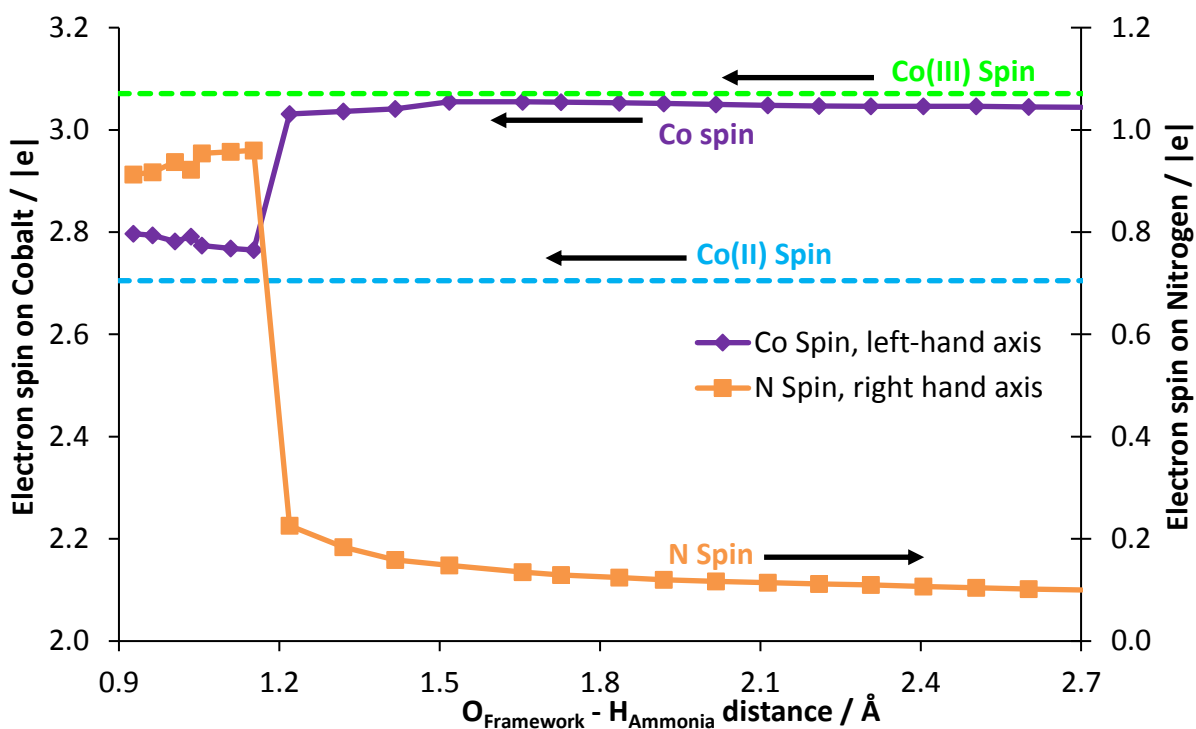


Figure S5: Spin evolution of bimetallic CoTiAlPO-5 for the activation of ammonia.

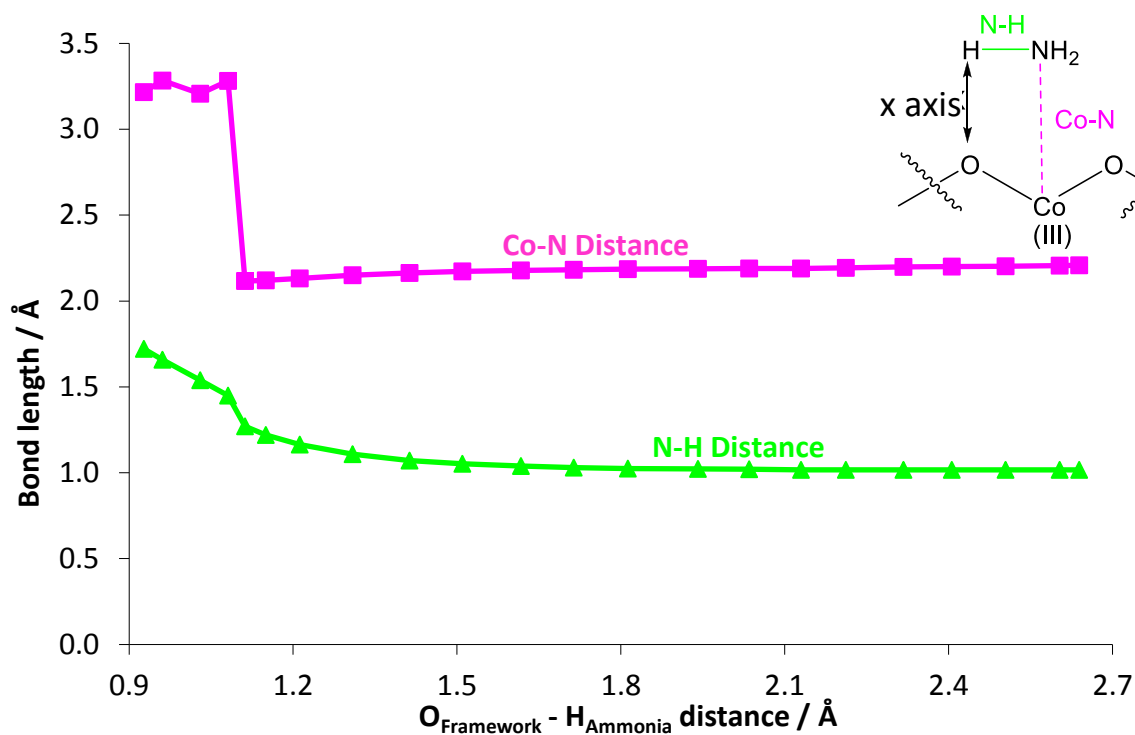


Figure S6: The evolution of bond lengths in the monometallic CoAlPO-5 system for the initial ammonia activation step.

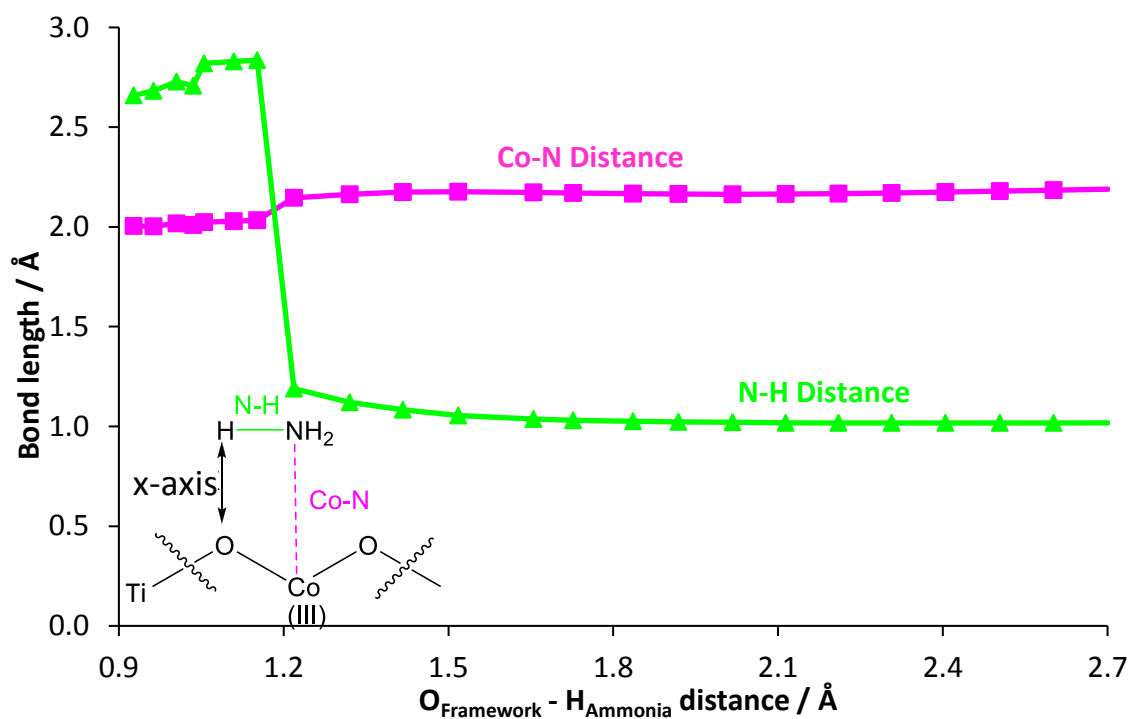


Figure S7: The evolution of bond lengths in the bimetallic CoTiAlPO-5 system for the initial ammonia activation step.

Oxygen addition step

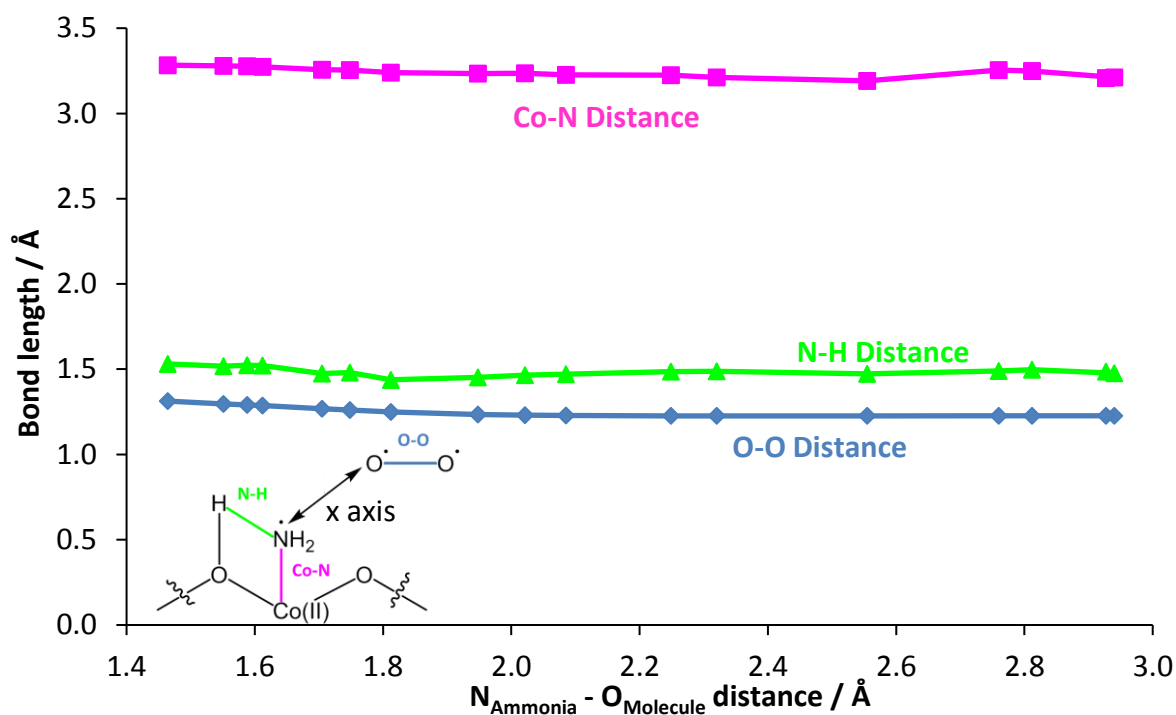


Figure S8: The evolution of bond lengths in the monometallic CoAlPO-5 system for the NH₂OO formation step.

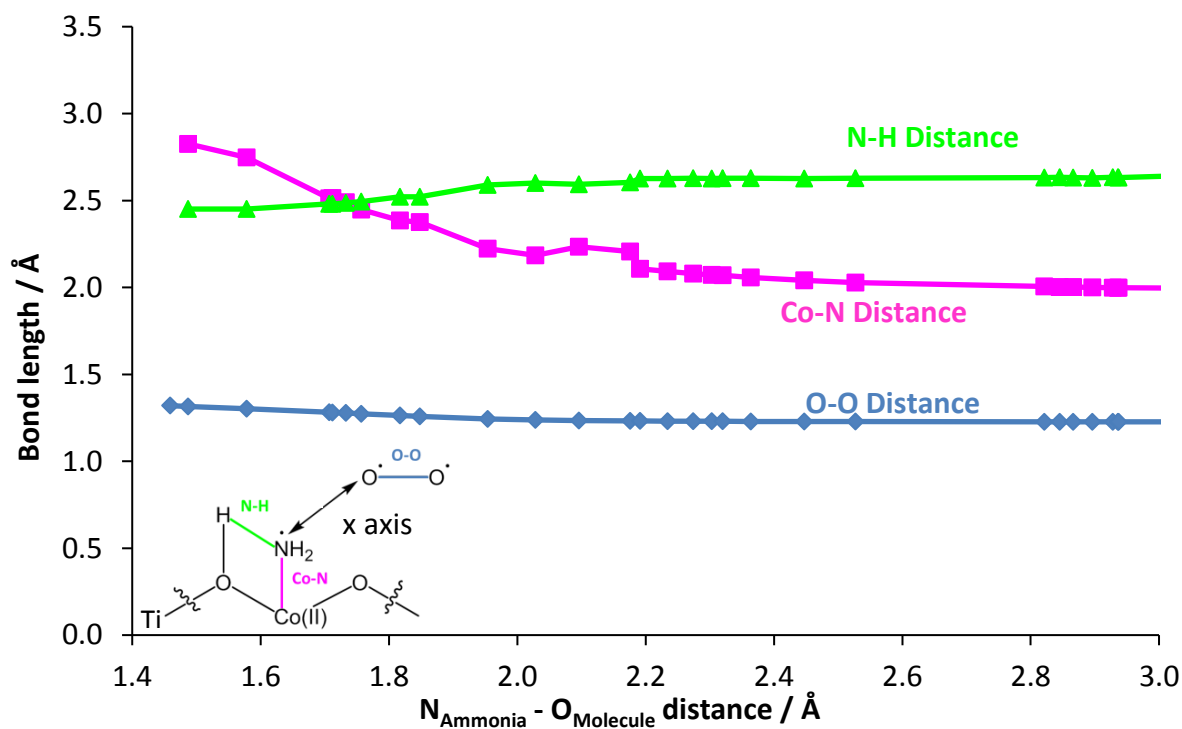


Figure S9: The evolution of bond lengths in the bimetallic CoTiAlPO-5 system for the NH₂OO formation step.

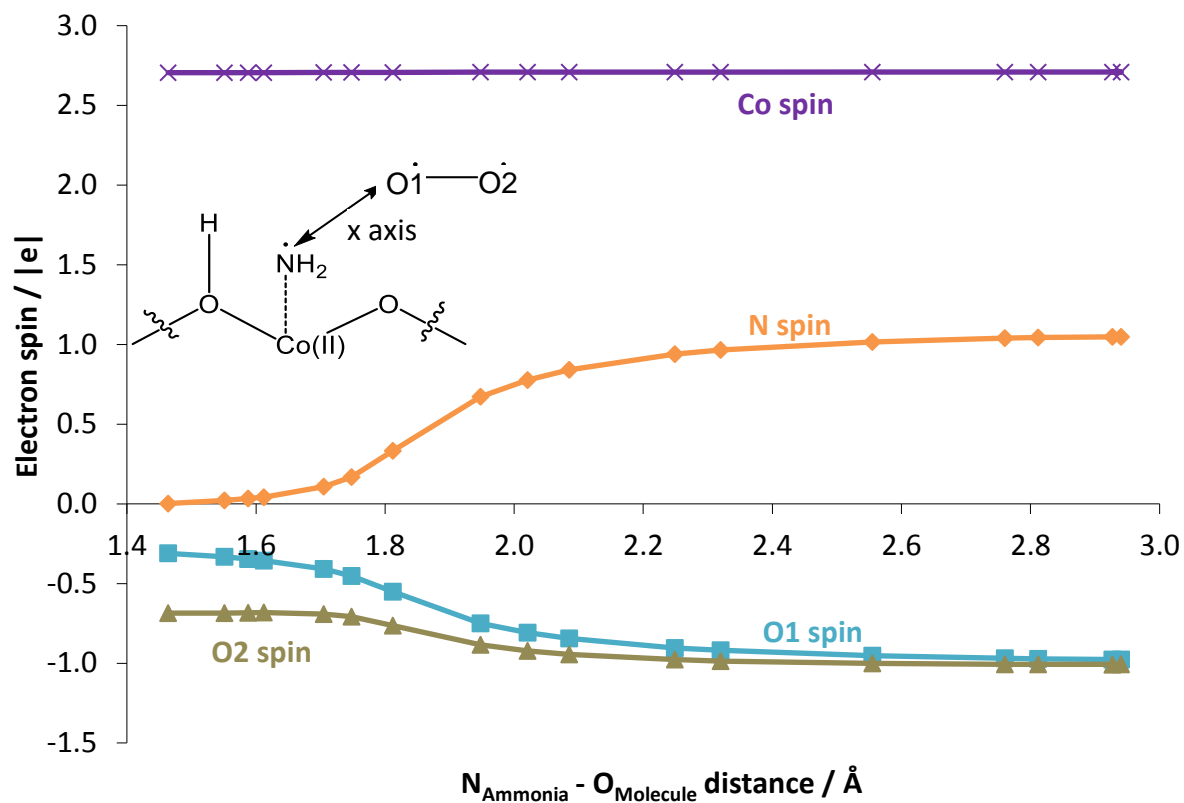


Figure S10: The evolution of spin in the monometallic CoAlPO-5 system for the formation of the NH₂OO radical species.

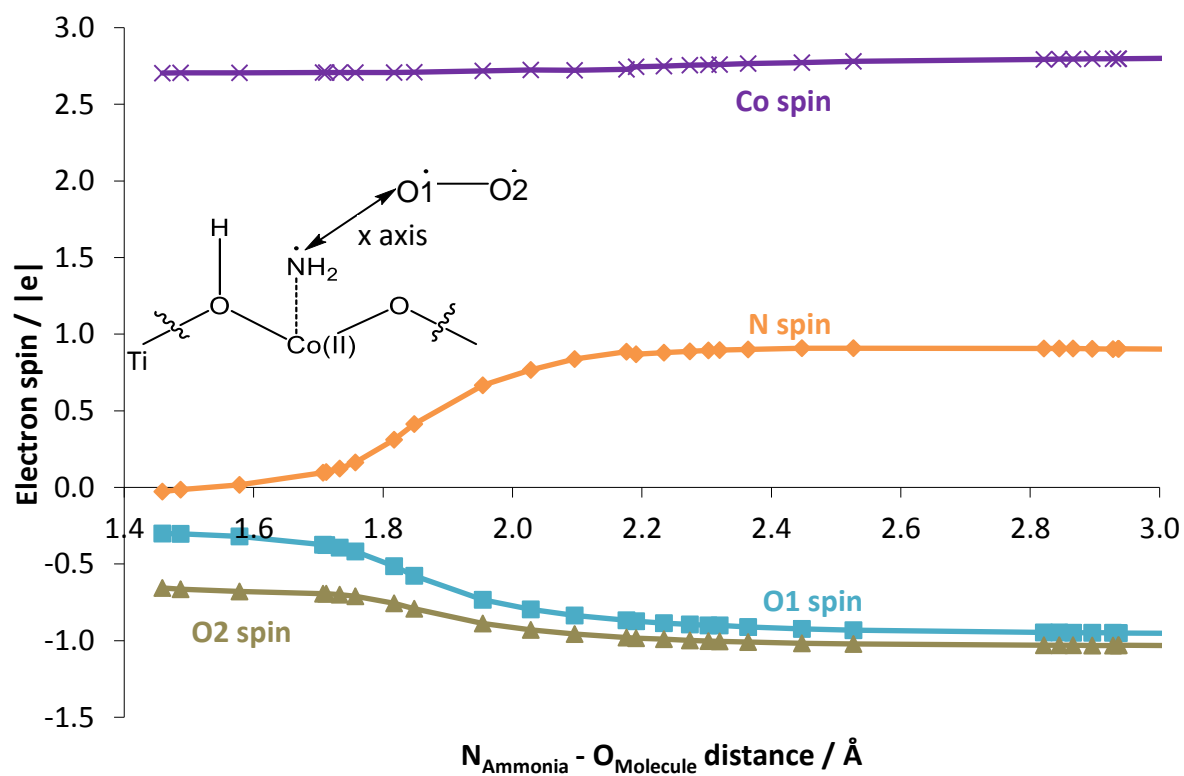


Figure S11: The evolution of spin in the bimetallic CoTiAlPO-5 system for the formation of the NH₂OO radical species

Transition state vibrational frequency calculations reported as they appear from the CRYSTAL output

Monometallic hydrogen abstraction step

MODES		EIGV (HARTREE**2)	FREQUENCIES (CM**1)	(THZ)	IRREP	IR	INTENS (KM/MOL)	RAMAN
1-	1	-0.2263E-06	-104.4045	-3.1300	(A)	A	(0.00)	A
2-	2	0.3989E-16	0.0000	0.0000	(A)	A	(0.00)	A
3-	3	0.2222E-15	0.0000	0.0000	(A)	A	(0.00)	A
4-	4	0.3864E-15	0.0000	0.0000	(A)	A	(0.00)	A
5-	5	0.3954E-08	13.8010	0.4137	(A)	A	(0.00)	A
6-	6	0.8744E-07	64.8980	1.9456	(A)	A	(0.00)	A
7-	7	0.9419E-07	67.3592	2.0194	(A)	A	(0.00)	A
8-	8	0.1445E-06	83.4420	2.5015	(A)	A	(0.00)	A
9-	9	0.1608E-06	88.0056	2.6383	(A)	A	(0.00)	A
10-	10	0.1647E-06	89.0673	2.6702	(A)	A	(0.00)	A
11-	11	0.1759E-06	92.0465	2.7595	(A)	A	(0.00)	A
12-	12	0.2085E-06	100.2263	3.0047	(A)	A	(0.00)	A
13-	13	0.2378E-06	107.0246	3.2085	(A)	A	(0.00)	A
14-	14	0.2564E-06	111.1421	3.3320	(A)	A	(0.00)	A
15-	15	0.2806E-06	116.2594	3.4854	(A)	A	(0.00)	A
16-	16	0.2897E-06	118.1342	3.5416	(A)	A	(0.00)	A
17-	17	0.3054E-06	121.2979	3.6364	(A)	A	(0.00)	A
18-	18	0.3144E-06	123.0580	3.6892	(A)	A	(0.00)	A
19-	19	0.3273E-06	125.5572	3.7641	(A)	A	(0.00)	A
20-	20	0.3623E-06	132.0988	3.9602	(A)	A	(0.00)	A
21-	21	0.3820E-06	135.6484	4.0666	(A)	A	(0.00)	A
22-	22	0.3944E-06	137.8362	4.1322	(A)	A	(0.00)	A
23-	23	0.4226E-06	142.6684	4.2771	(A)	A	(0.00)	A
24-	24	0.4420E-06	145.9165	4.3745	(A)	A	(0.00)	A
25-	25	0.4877E-06	153.2678	4.5949	(A)	A	(0.00)	A
26-	26	0.5023E-06	155.5505	4.6633	(A)	A	(0.00)	A
27-	27	0.5248E-06	159.0003	4.7667	(A)	A	(0.00)	A
28-	28	0.5629E-06	164.6584	4.9363	(A)	A	(0.00)	A
29-	29	0.5723E-06	166.0349	4.9776	(A)	A	(0.00)	A
30-	30	0.5949E-06	169.2856	5.0751	(A)	A	(0.00)	A
31-	31	0.6228E-06	173.2041	5.1925	(A)	A	(0.00)	A
32-	32	0.6310E-06	174.3420	5.2266	(A)	A	(0.00)	A
33-	33	0.6677E-06	179.3418	5.3765	(A)	A	(0.00)	A
34-	34	0.6907E-06	182.3956	5.4681	(A)	A	(0.00)	A
35-	35	0.7043E-06	184.1846	5.5217	(A)	A	(0.00)	A
36-	36	0.7665E-06	192.1544	5.7606	(A)	A	(0.00)	A
37-	37	0.7937E-06	195.5323	5.8619	(A)	A	(0.00)	A
38-	38	0.8130E-06	197.8873	5.9325	(A)	A	(0.00)	A
39-	39	0.8274E-06	199.6357	5.9849	(A)	A	(0.00)	A
40-	40	0.8438E-06	201.6041	6.0439	(A)	A	(0.00)	A
41-	41	0.8690E-06	204.5911	6.1335	(A)	A	(0.00)	A
42-	42	0.9030E-06	208.5604	6.2525	(A)	A	(0.00)	A
43-	43	0.9256E-06	211.1515	6.3302	(A)	A	(0.00)	A
44-	44	0.9542E-06	214.3902	6.4273	(A)	A	(0.00)	A
45-	45	0.9650E-06	215.5993	6.4635	(A)	A	(0.00)	A
46-	46	0.1014E-05	221.0204	6.6260	(A)	A	(0.00)	A
47-	47	0.1027E-05	222.3889	6.6671	(A)	A	(0.00)	A
48-	48	0.1048E-05	224.6988	6.7363	(A)	A	(0.00)	A
49-	49	0.1095E-05	229.6950	6.8861	(A)	A	(0.00)	A
50-	50	0.1113E-05	231.5379	6.9413	(A)	A	(0.00)	A
51-	51	0.1153E-05	235.7121	7.0665	(A)	A	(0.00)	A
52-	52	0.1197E-05	240.1530	7.1996	(A)	A	(0.00)	A
53-	53	0.1225E-05	242.9128	7.2823	(A)	A	(0.00)	A
54-	54	0.1260E-05	246.3567	7.3856	(A)	A	(0.00)	A
55-	55	0.1294E-05	249.6375	7.4839	(A)	A	(0.00)	A
56-	56	0.1367E-05	256.6213	7.6933	(A)	A	(0.00)	A
57-	57	0.1433E-05	262.7253	7.8763	(A)	A	(0.00)	A
58-	58	0.1464E-05	265.5110	7.9598	(A)	A	(0.00)	A
59-	59	0.1481E-05	267.0562	8.0061	(A)	A	(0.00)	A
60-	60	0.1535E-05	271.9355	8.1524	(A)	A	(0.00)	A
61-	61	0.1554E-05	273.6323	8.2033	(A)	A	(0.00)	A
62-	62	0.1580E-05	275.9137	8.2717	(A)	A	(0.00)	A
63-	63	0.1623E-05	279.6203	8.3828	(A)	A	(0.00)	A
64-	64	0.1682E-05	284.6598	8.5339	(A)	A	(0.00)	A
65-	65	0.1700E-05	286.1828	8.5795	(A)	A	(0.00)	A
66-	66	0.1783E-05	293.8579	8.8096	(A)	A	(0.00)	A
67-	67	0.1932E-05	305.0999	9.1467	(A)	A	(0.00)	A
68-	68	0.1969E-05	307.8836	9.2301	(A)	A	(0.00)	A
69-	69	0.2018E-05	311.7467	9.3459	(A)	A	(0.00)	A
70-	70	0.2081E-05	316.6067	9.4916	(A)	A	(0.00)	A
71-	71	0.2104E-05	318.3263	9.5432	(A)	A	(0.00)	A
72-	72	0.2245E-05	328.8471	9.8586	(A)	A	(0.00)	A
73-	73	0.2361E-05	337.2430	10.1103	(A)	A	(0.00)	A
74-	74	0.2488E-05	346.2166	10.3793	(A)	A	(0.00)	A
75-	75	0.2497E-05	346.8343	10.3978	(A)	A	(0.00)	A
76-	76	0.2602E-05	354.0100	10.6130	(A)	A	(0.00)	A
77-	77	0.2755E-05	364.2947	10.9213	(A)	A	(0.00)	A
78-	78	0.2859E-05	371.0880	11.1249	(A)	A	(0.00)	A
79-	79	0.2936E-05	376.0546	11.2738	(A)	A	(0.00)	A
80-	80	0.2971E-05	378.3206	11.3418	(A)	A	(0.00)	A
81-	81	0.3001E-05	380.2122	11.3985	(A)	A	(0.00)	A
82-	82	0.3069E-05	384.4604	11.5258	(A)	A	(0.00)	A
83-	83	0.3108E-05	386.9123	11.5993	(A)	A	(0.00)	A
84-	84	0.3131E-05	388.3413	11.6422	(A)	A	(0.00)	A
85-	85	0.3170E-05	390.7693	11.7150	(A)	A	(0.00)	A
86-	86	0.3247E-05	395.5113	11.8571	(A)	A	(0.00)	A
87-	87	0.3349E-05	401.6331	12.0407	(A)	A	(0.00)	A
88-	88	0.3387E-05	403.9166	12.1091	(A)	A	(0.00)	A
89-	89	0.3443E-05	407.2158	12.2080	(A)	A	(0.00)	A
90-	90	0.3489E-05	409.9641	12.2904	(A)	A	(0.00)	A
91-	91	0.3530E-05	412.3655	12.3624	(A)	A	(0.00)	A
92-	92	0.3593E-05	416.0268	12.4722	(A)	A	(0.00)	A
93-	93	0.3678E-05	420.8985	12.6182	(A)	A	(0.00)	A
94-	94	0.3701E-05	422.2402	12.6584	(A)	A	(0.00)	A
95-	95	0.3736E-05	424.2245	12.7179	(A)	A	(0.00)	A
96-	96	0.3780E-05	426.7301	12.7930	(A)	A	(0.00)	A
97-	97	0.3848E-05	430.5093	12.9063	(A)	A	(0.00)	A
98-	98	0.3926E-05	434.8743	13.0372	(A)	A	(0.00)	A
99-	99	0.3949E-05	436.0965	13.0738	(A)	A	(0.00)	A
100-	100	0.4056E-05	442.0201	13.2514	(A)	A	(0.00)	A
101-	101	0.4085E-05	443.5947	13.2986	(A)	A	(0.00)	A

102-	102	0.421E-05	450.3466	13.5011	(A)	A	(0.00)	A
103-	103	0.432E-05	456.1998	13.6765	(A)	A	(0.00)	A
104-	104	0.437E-05	458.8744	13.7567	(A)	A	(0.00)	A
105-	105	0.443A-05	462.1347	13.8545	(A)	A	(0.00)	A
106-	106	0.4507E-05	465.9507	13.9689	(A)	A	(0.00)	A
107-	107	0.4534E-05	467.3300	14.0102	(A)	A	(0.00)	A
108-	108	0.4624E-05	471.9723	14.1494	(A)	A	(0.00)	A
109-	109	0.4687E-05	475.1536	14.2447	(A)	A	(0.00)	A
110-	110	0.4744E-05	478.0305	14.3310	(A)	A	(0.00)	A
111-	111	0.4837E-05	482.7013	14.4710	(A)	A	(0.00)	A
112-	112	0.4917E-05	486.6587	14.5897	(A)	A	(0.00)	A
113-	113	0.4984E-05	489.9512	14.6884	(A)	A	(0.00)	A
114-	114	0.5066E-05	494.0020	14.8098	(A)	A	(0.00)	A
115-	115	0.5163E-05	498.6894	14.9503	(A)	A	(0.00)	A
116-	116	0.5173E-05	499.1730	14.9648	(A)	A	(0.00)	A
117-	117	0.5275E-05	504.0751	15.1118	(A)	A	(0.00)	A
118-	118	0.5280E-05	504.3342	15.1196	(A)	A	(0.00)	A
119-	119	0.5344E-05	507.3850	15.2110	(A)	A	(0.00)	A
120-	120	0.5434E-05	511.6171	15.3379	(A)	A	(0.00)	A
121-	121	0.5486E-05	516.8773	15.4956	(A)	A	(0.00)	A
122-	122	0.5764E-05	526.9382	15.7972	(A)	A	(0.00)	A
123-	123	0.5870E-05	531.7645	15.9419	(A)	A	(0.00)	A
124-	124	0.6068E-05	540.6528	16.2084	(A)	A	(0.00)	A
125-	125	0.6159E-05	544.6631	16.3286	(A)	A	(0.00)	A
126-	126	0.6223E-05	547.5007	16.4137	(A)	A	(0.00)	A
127-	127	0.6457E-05	557.6860	16.7190	(A)	A	(0.00)	A
128-	128	0.6584E-05	563.1710	16.8834	(A)	A	(0.00)	A
129-	129	0.6697E-05	567.9576	17.0269	(A)	A	(0.00)	A
130-	130	0.6919E-05	577.3209	17.3076	(A)	A	(0.00)	A
131-	131	0.6949E-05	578.5703	17.3451	(A)	A	(0.00)	A
132-	132	0.7119E-05	585.5718	17.5550	(A)	A	(0.00)	A
133-	133	0.7179E-05	588.0434	17.6291	(A)	A	(0.00)	A
134-	134	0.7384E-05	596.4005	17.8796	(A)	A	(0.00)	A
135-	135	0.7469E-05	599.8206	17.9822	(A)	A	(0.00)	A
136-	136	0.7597E-05	604.9299	18.1353	(A)	A	(0.00)	A
137-	137	0.8390E-05	635.7041	19.0579	(A)	A	(0.00)	A
138-	138	0.8637E-05	644.9910	19.3363	(A)	A	(0.00)	A
139-	139	0.8992E-05	658.1197	19.7299	(A)	A	(0.00)	A
140-	140	0.9217E-05	666.3077	19.9754	(A)	A	(0.00)	A
141-	141	0.9354E-05	671.2408	20.1233	(A)	A	(0.00)	A
142-	142	0.9414E-05	673.4019	20.1881	(A)	A	(0.00)	A
143-	143	0.9565E-05	678.7936	20.3497	(A)	A	(0.00)	A
144-	144	0.9777E-05	686.2678	20.7338	(A)	A	(0.00)	A
145-	145	0.9843E-05	688.5788	20.6431	(A)	A	(0.00)	A
146-	146	0.1016E-04	699.5900	20.9732	(A)	A	(0.00)	A
147-	147	0.1045E-04	709.4631	21.2692	(A)	A	(0.00)	A
148-	148	0.1063E-04	715.5943	21.4530	(A)	A	(0.00)	A
149-	149	0.1110E-04	731.3179	21.9244	(A)	A	(0.00)	A
150-	150	0.1121E-04	734.9410	22.0330	(A)	A	(0.00)	A
151-	151	0.1130E-04	737.8679	22.1207	(A)	A	(0.00)	A
152-	152	0.1147E-04	743.4379	22.2877	(A)	A	(0.00)	A
153-	153	0.1153E-04	745.1407	22.3389	(A)	A	(0.00)	A
154-	154	0.1170E-04	750.7958	22.5083	(A)	A	(0.00)	A
155-	155	0.1178E-04	753.2721	22.5825	(A)	A	(0.00)	A
156-	156	0.1191E-04	757.4294	22.7072	(A)	A	(0.00)	A
157-	157	0.1193E-04	758.1668	22.7293	(A)	A	(0.00)	A
158-	158	0.1208E-04	762.8729	22.8704	(A)	A	(0.00)	A
159-	159	0.1217E-04	765.7977	22.9580	(A)	A	(0.00)	A
160-	160	0.1233E-04	770.6570	23.1037	(A)	A	(0.00)	A
161-	161	0.1237E-04	771.9066	23.1412	(A)	A	(0.00)	A
162-	162	0.1239E-04	772.5213	23.1956	(A)	A	(0.00)	A
163-	163	0.1253E-04	776.9494	23.2925	(A)	A	(0.00)	A
164-	164	0.1260E-04	779.1274	23.3577	(A)	A	(0.00)	A
165-	165	0.1282E-04	785.7549	23.5563	(A)	A	(0.00)	A
166-	166	0.1284E-04	786.5430	23.5800	(A)	A	(0.00)	A
167-	167	0.1294E-04	789.3817	23.6651	(A)	A	(0.00)	A
168-	168	0.1308E-04	791.6688	23.7343	(A)	A	(0.00)	A
169-	169	0.1308E-04	793.7373	23.7955	(A)	A	(0.00)	A
170-	170	0.1317E-04	796.3757	23.8747	(A)	A	(0.00)	A
171-	171	0.1344E-04	804.4930	24.1811	(A)	A	(0.00)	A
172-	172	0.1350E-04	806.3275	24.1731	(A)	A	(0.00)	A
173-	173	0.1392E-04	818.8229	24.5777	(A)	A	(0.00)	A
174-	174	0.1444E-04	833.8751	24.9889	(A)	A	(0.00)	A
175-	175	0.221E-04	1034.0143	31.1008	(A)	A	(0.00)	A
176-	176	0.2385E-04	1071.3235	32.1355	(A)	A	(0.00)	A
177-	177	0.2536E-04	1105.9276	33.1369	(A)	A	(0.00)	A
178-	178	0.2566E-04	1109.6133	33.2654	(A)	A	(0.00)	A
179-	179	0.2579E-04	1114.5495	33.4134	(A)	A	(0.00)	A
180-	180	0.2593E-04	1117.6407	33.5660	(A)	A	(0.00)	A
181-	181	0.2623E-04	1123.9914	33.6964	(A)	A	(0.00)	A
182-	182	0.2627E-04	1124.9642	33.7255	(A)	A	(0.00)	A
183-	183	0.2638E-04	1127.3475	33.7970	(A)	A	(0.00)	A
184-	184	0.2647E-04	1129.1680	33.8516	(A)	A	(0.00)	A
185-	185	0.2648E-04	1129.3214	33.8562	(A)	A	(0.00)	A
186-	186	0.2657E-04	1131.3008	33.9155	(A)	A	(0.00)	A
187-	187	0.2683E-04	1136.7855	34.0800	(A)	A	(0.00)	A
188-	188	0.2692E-04	1138.7256	34.1381	(A)	A	(0.00)	A
189-	189	0.2695E-04	1139.2744	34.1546	(A)	A	(0.00)	A
190-	190	0.2701E-04	1140.7660	34.1975	(A)	A	(0.00)	A
191-	191	0.2707E-04	1141.9752	34.2356	(A)	A	(0.00)	A
192-	192	0.2714E-04	1143.4871	34.2806	(A)	A	(0.00)	A
193-	193	0.2723E-04	1145.2248	34.3330	(A)	A	(0.00)	A
194-	194	0.2730E-04	1146.6374	34.3753	(A)	A	(0.00)	A
195-	195	0.2742E-04	1149.2684	34.4542	(A)	A	(0.00)	A
196-	196	0.2757E-04	1152.3837	34.5477	(A)	A	(0.00)	A
197-	197	0.2764E-04	1153.8339	34.5911	(A)	A	(0.00)	A
198-	198	0.2766E-04	1154.3012	34.6051	(A)	A	(0.00)	A
199-	199	0.2784E-04	1157.9953	34.7158	(A)	A	(0.00)	A
200-	200	0.2800E-04	1161.2748	34.8141	(A)	A	(0.00)	A
201-	201	0.2805E-04	1162.3642	34.8467	(A)	A	(0.00)	A
202-	202	0.2811E-04	1163.5902	34.8834	(A)	A	(0.00)	A
203-	203	0.2828E-04	1166.4933	34.9813	(A)	A	(0.00)	A
204-	204	0.2827E-04	1166.8498	34.9813	(A)	A	(0.00)	A
205-	205	0.2837E-04	1169.0532	35.0473	(A)	A	(0.00)	A
206-	206	0.2850E-04	1171.6700	35.1258	(A)	A	(0.00)	A
207-	207	0.2850E-04	1172.0547	35.1373	(A)	A	(0.00)	A
208-	208	0.2870E-04	1175.7426	35.2479	(A)	A	(0.00)	A
209-	209	0.2892E-04	1180.2552	35.3832	(A)	A	(0.00)	A
210-	210	0.2896E-04	1181.0470	35.4069	(A)	A	(0.00)	A
211-	211	0.2913E-04	1184.5970	35.5333	(A)	A	(0.00)	A
212-	212	0.3179E-04	1237.4491	37.0198	(A)	A	(0.00)	A

213- 213	0.3206E-04	1242.6999	37.2552	(A)	A (0.00)	A
214- 214	0.3252E-04	1251.4944	37.5189	(A)	A (0.00)	A
215- 215	0.3275E-04	1255.9233	37.6516	(A)	A (0.00)	A
216- 216	0.3278E-04	1256.5068	37.6691	(A)	A (0.00)	A
217- 217	0.3287E-04	1258.2679	37.7219	(A)	A (0.00)	A
218- 218	0.3325E-04	1265.4788	37.9381	(A)	A (0.00)	A
219- 219	0.3347E-04	1269.7789	38.0670	(A)	A (0.00)	A
220- 220	0.3375E-04	1274.9431	38.2218	(A)	A (0.00)	A
221- 221	0.3391E-04	1278.1378	38.3176	(A)	A (0.00)	A
222- 222	0.3427E-04	1284.7597	38.5161	(A)	A (0.00)	A
223- 223	0.3456E-04	1290.2400	38.6804	(A)	A (0.00)	A
224- 224	0.4318E-04	1442.2241	43.2368	(A)	A (0.00)	A
225- 225	0.5580E-04	1639.4200	49.1486	(A)	A (0.00)	A
226- 226	0.7061E-04	1844.2687	55.2898	(A)	A (0.00)	A
227- 227	0.2632E-03	3560.7146	106.7475	(A)	A (0.00)	A
228- 228	0.2789E-03	3671.3545	110.0644	(A)	A (0.00)	A

Bimetallic hydrogen abstraction step

MODES	E (HARTREE*E2)	FREQUENCIES (CM-1)	(THZ)	IRREP	IR	INTENS (KM/MOL)	RAMAN
1- 1	-0.2288E-07	-33.1991	-0.9953	(A)	A (0.00)	A
2- 2	-0.2827E-16	0.0000	0.0000	(A)	A (0.00)	A
3- 3	0.1521E-16	0.0000	0.0000	(A)	A (0.00)	A
4- 4	0.6593E-16	0.0000	0.0000	(A)	A (0.00)	A
5- 5	0.7579E-07	60.4222	1.8114	(A)	A (0.00)	A
6- 6	0.9525E-07	67.7341	2.0306	(A)	A (0.00)	A
7- 7	0.1105E-06	72.9451	2.1868	(A)	A (0.00)	A
8- 8	0.1401E-06	82.1353	2.4624	(A)	A (0.00)	A
9- 9	0.1573E-06	87.0479	2.6096	(A)	A (0.00)	A
10- 10	0.1719E-06	90.9951	2.7280	(A)	A (0.00)	A
11- 11	0.1772E-06	92.3904	2.7698	(A)	A (0.00)	A
12- 12	0.2133E-06	101.3611	3.0387	(A)	A (0.00)	A
13- 13	0.2339E-06	106.1480	3.1822	(A)	A (0.00)	A
14- 14	0.2505E-06	109.8577	3.2935	(A)	A (0.00)	A
15- 15	0.2689E-06	113.8115	3.4120	(A)	A (0.00)	A
16- 16	0.2772E-06	115.5531	3.4642	(A)	A (0.00)	A
17- 17	0.2835E-06	116.8648	3.5035	(A)	A (0.00)	A
18- 18	0.2893E-06	118.0481	3.5390	(A)	A (0.00)	A
19- 19	0.3151E-06	123.2048	3.6936	(A)	A (0.00)	A
20- 20	0.3329E-06	126.6388	3.7965	(A)	A (0.00)	A
21- 21	0.3518E-06	130.1723	3.9025	(A)	A (0.00)	A
22- 22	0.3740E-06	134.2130	4.0236	(A)	A (0.00)	A
23- 23	0.3908E-06	137.2102	4.1135	(A)	A (0.00)	A
24- 24	0.4093E-06	140.4194	4.2097	(A)	A (0.00)	A
25- 25	0.4272E-06	143.4463	4.3004	(A)	A (0.00)	A
26- 26	0.4670E-06	149.9775	4.4962	(A)	A (0.00)	A
27- 27	0.4741E-06	151.1143	4.5303	(A)	A (0.00)	A
28- 28	0.5024E-06	155.5653	4.6637	(A)	A (0.00)	A
29- 29	0.5266E-06	159.2661	4.7747	(A)	A (0.00)	A
30- 30	0.5341E-06	160.3933	4.8085	(A)	A (0.00)	A
31- 31	0.5492E-06	162.6480	4.8761	(A)	A (0.00)	A
32- 32	0.5541E-06	163.3783	4.8980	(A)	A (0.00)	A
33- 33	0.5863E-06	168.0573	5.0382	(A)	A (0.00)	A
34- 34	0.6286E-06	174.0038	5.2165	(A)	A (0.00)	A
35- 35	0.6613E-06	178.4756	5.3506	(A)	A (0.00)	A
36- 36	0.6755E-06	180.3810	5.4077	(A)	A (0.00)	A
37- 37	0.7147E-06	185.5383	5.5623	(A)	A (0.00)	A
38- 38	0.7550E-06	190.7059	5.7172	(A)	A (0.00)	A
39- 39	0.7738E-06	193.0631	5.7879	(A)	A (0.00)	A
40- 40	0.7855E-06	194.5152	5.8314	(A)	A (0.00)	A
41- 41	0.8111E-06	197.6669	5.9259	(A)	A (0.00)	A
42- 42	0.8400E-06	201.1561	6.0305	(A)	A (0.00)	A
43- 43	0.8551E-06	202.9517	6.0843	(A)	A (0.00)	A
44- 44	0.8934E-06	207.4433	6.2190	(A)	A (0.00)	A
45- 45	0.9366E-06	212.4041	6.3677	(A)	A (0.00)	A
46- 46	0.9638E-06	215.4687	6.4596	(A)	A (0.00)	A
47- 47	0.9842E-06	217.7353	6.5275	(A)	A (0.00)	A
48- 48	0.1027E-05	222.4378	6.6685	(A)	A (0.00)	A
49- 49	0.1039E-05	223.7516	6.7079	(A)	A (0.00)	A
50- 50	0.1061E-05	226.0592	6.7771	(A)	A (0.00)	A
51- 51	0.1091E-05	229.2245	6.8720	(A)	A (0.00)	A
52- 52	0.1137E-05	234.0042	7.0153	(A)	A (0.00)	A
53- 53	0.1208E-05	241.1737	7.2302	(A)	A (0.00)	A
54- 54	0.1239E-05	244.2813	7.3234	(A)	A (0.00)	A
55- 55	0.1264E-05	246.7849	7.3984	(A)	A (0.00)	A
56- 56	0.1295E-05	249.7146	7.4863	(A)	A (0.00)	A
57- 57	0.1305E-05	250.7259	7.5166	(A)	A (0.00)	A
58- 58	0.1344E-05	254.3988	7.6267	(A)	A (0.00)	A
59- 59	0.1366E-05	256.5073	7.6899	(A)	A (0.00)	A
60- 60	0.1389E-05	258.6496	7.7541	(A)	A (0.00)	A
61- 61	0.1458E-05	265.0357	7.9456	(A)	A (0.00)	A
62- 62	0.1508E-05	269.5235	8.0801	(A)	A (0.00)	A
63- 63	0.1542E-05	272.5184	8.1699	(A)	A (0.00)	A
64- 64	0.1580E-05	275.9045	8.2714	(A)	A (0.00)	A
65- 65	0.1600E-05	277.6579	8.3240	(A)	A (0.00)	A
66- 66	0.1657E-05	282.5290	8.4700	(A)	A (0.00)	A
67- 67	0.1770E-05	291.9800	8.7533	(A)	A (0.00)	A
68- 68	0.1805E-05	294.8521	8.8394	(A)	A (0.00)	A
69- 69	0.1871E-05	300.1795	8.9992	(A)	A (0.00)	A
70- 70	0.1904E-05	302.8806	9.0801	(A)	A (0.00)	A
71- 71	0.1953E-05	306.7107	9.1950	(A)	A (0.00)	A
72- 72	0.2044E-05	313.8166	9.4080	(A)	A (0.00)	A
73- 73	0.2134E-05	320.5899	9.6110	(A)	A (0.00)	A
74- 74	0.2199E-05	325.4940	9.7581	(A)	A (0.00)	A
75- 75	0.2249E-05	329.1114	9.8665	(A)	A (0.00)	A
76- 76	0.2331E-05	335.0725	10.0452	(A)	A (0.00)	A
77- 77	0.2456E-05	343.9669	10.3119	(A)	A (0.00)	A
78- 78	0.2482E-05	345.7678	10.3659	(A)	A (0.00)	A
79- 79	0.2610E-05	354.5565	10.6293	(A)	A (0.00)	A
80- 80	0.2715E-05	361.6505	10.8420	(A)	A (0.00)	A
81- 81	0.2806E-05	367.6371	11.0215	(A)	A (0.00)	A
82- 82	0.2826E-05	368.9531	11.0609	(A)	A (0.00)	A
83- 83	0.2887E-05	372.9268	11.1801	(A)	A (0.00)	A
84- 84	0.2979E-05	378.7816	11.3556	(A)	A (0.00)	A
85- 85	0.3041E-05	382.7520	11.4746	(A)	A (0.00)	A
86- 86	0.3073E-05	384.7191	11.5336	(A)	A (0.00)	A
87- 87	0.3159E-05	390.0786	11.6943	(A)	A (0.00)	A

88- 88	0.3190E-05	391.9869	11.7515	(A)	A (0.00)	A
89- 89	0.3223E-05	394.0081	11.8121	(A)	A (0.00)	A
90- 90	0.3253E-05	395.8386	11.8669	(A)	A (0.00)	A
91- 91	0.3296E-05	398.4618	11.9456	(A)	A (0.00)	A
92- 92	0.3439E-05	406.9905	12.2013	(A)	A (0.00)	A
93- 93	0.3500E-05	410.6090	12.3097	(A)	A (0.00)	A
94- 94	0.3627E-05	417.9692	12.5304	(A)	A (0.00)	A
95- 95	0.3634E-05	418.3784	12.5427	(A)	A (0.00)	A
96- 96	0.3692E-05	421.6927	12.6420	(A)	A (0.00)	A
97- 97	0.3716E-05	423.0785	12.6836	(A)	A (0.00)	A
98- 98	0.3776E-05	426.4552	12.7848	(A)	A (0.00)	A
99- 99	0.3826E-05	429.3203	12.8707	(A)	A (0.00)	A
100- 100	0.3899E-05	433.3662	12.9920	(A)	A (0.00)	A
101- 101	0.3990E-05	438.4159	13.1434	(A)	A (0.00)	A
102- 102	0.4102E-05	444.4901	13.3255	(A)	A (0.00)	A
103- 103	0.4129E-05	445.9778	13.3701	(A)	A (0.00)	A
104- 104	0.4205E-05	450.0823	13.4931	(A)	A (0.00)	A
105- 105	0.4252E-05	452.5705	13.5677	(A)	A (0.00)	A
106- 106	0.4298E-05	455.0030	13.6406	(A)	A (0.00)	A
107- 107	0.4403E-05	460.5511	13.8070	(A)	A (0.00)	A
108- 108	0.4500E-05	465.5755	13.9576	(A)	A (0.00)	A
109- 109	0.4540E-05	467.6491	14.0198	(A)	A (0.00)	A
110- 110	0.4566E-05	468.9544	14.0589	(A)	A (0.00)	A
111- 111	0.4671E-05	474.3538	14.2208	(A)	A (0.00)	A
112- 112	0.4738E-05	477.7463	14.3225	(A)	A (0.00)	A
113- 113	0.4802E-05	480.9506	14.4185	(A)	A (0.00)	A
114- 114	0.4833E-05	482.4856	14.4646	(A)	A (0.00)	A
115- 115	0.4885E-05	485.1038	14.5430	(A)	A (0.00)	A
116- 116	0.4961E-05	488.8423	14.6551	(A)	A (0.00)	A
117- 117	0.4967E-05	489.1469	14.6643	(A)	A (0.00)	A
118- 118	0.4999E-05	490.7002	14.7108	(A)	A (0.00)	A
119- 119	0.5101E-05	495.6912	14.8604	(A)	A (0.00)	A
120- 120	0.5125E-05	496.8364	14.8948	(A)	A (0.00)	A
121- 121	0.5312E-05	505.8280	15.1643	(A)	A (0.00)	A
122- 122	0.5392E-05	509.6420	15.2787	(A)	A (0.00)	A
123- 123	0.5481E-05	513.8367	15.4044	(A)	A (0.00)	A
124- 124	0.5650E-05	521.7049	15.6403	(A)	A (0.00)	A
125- 125	0.5823E-05	529.5940	15.8768	(A)	A (0.00)	A
126- 126	0.5937E-05	534.7651	16.0319	(A)	A (0.00)	A
127- 127	0.5964E-05	535.9672	16.0679	(A)	A (0.00)	A
128- 128	0.6167E-05	545.0321	16.3397	(A)	A (0.00)	A
129- 129	0.6294E-05	550.6001	16.5066	(A)	A (0.00)	A
130- 130	0.6542E-05	561.3537	16.8290	(A)	A (0.00)	A
131- 131	0.6682E-05	567.3328	17.0082	(A)	A (0.00)	A
132- 132	0.6699E-05	568.0465	17.0296	(A)	A (0.00)	A
133- 133	0.6840E-05	574.0092	17.2084	(A)	A (0.00)	A
134- 134	0.7004E-05	580.8470	17.4134	(A)	A (0.00)	A
135- 135	0.7062E-05	583.2577	17.4856	(A)	A (0.00)	A
136- 136	0.7266E-05	591.5998	17.7357	(A)	A (0.00)	A
137- 137	0.7340E-05	594.6175	17.8262	(A)	A (0.00)	A
138- 138	0.7628E-05	606.1823	18.1729	(A)	A (0.00)	A
139- 139	0.8008E-05	621.0929	18.6199	(A)	A (0.00)	A
140- 140	0.8148E-05	626.4975	18.7819	(A)	A (0.00)	A
141- 141	0.8233E-05	629.7540	18.8795	(A)	A (0.00)	A
142- 142	0.8487E-05	638.3902	19.1684	(A)	A (0.00)	A
143- 143	0.8978E-05	657.6072	19.7146	(A)	A (0.00)	A
144- 144	0.9101E-05	662.1042	19.8494	(A)	A (0.00)	A
145- 145	0.9206E-05	665.9801	19.9634	(A)	A (0.00)	A
146- 146	0.9515E-05	677.0658	20.2961	(A)	A (0.00)	A
147- 147	0.9678E-05	682.7880	20.4694	(A)	A (0.00)	A
148- 148	0.1009E-04	697.2760	20.9038	(A)	A (0.00)	A
149- 149	0.1021E-04	701.1310	21.0194	(A)	A (0.00)	A
150- 150	0.1055E-04	706.2387	21.2393	(A)	A (0.00)	A
151- 151	0.1065E-04	716.2834	21.4736	(A)	A (0.00)	A
152- 152	0.1079E-04	720.7715	21.6082	(A)	A (0.00)	A
153- 153	0.1082E-04	721.8170	21.6395	(A)	A (0.00)	A
154- 154	0.1105E-04	729.1760	21.8763	(A)	A (0.00)	A
155- 155	0.1125E-04	736.1083	22.0680	(A)	A (0.00)	A
156- 156	0.1146E-04	743.0284	22.2754	(A)	A (0.00)	A
157- 157	0.1159E-04	747.2529	22.4021	(A)	A (0.00)	A
158- 158	0.1165E-04	748.9887	22.4541	(A)	A (0.00)	A
159- 159	0.1168E-04	750.0194	22.4850	(A)	A (0.00)	A
160- 160	0.1173E-04	751.7484	22.5368	(A)	A (0.00)	A
161- 161	0.1193E-04	758.1971	22.7302	(A)	A (0.00)	A
162- 162	0.1198E-04	759.6531	22.7738	(A)	A (0.00)	A
163- 163	0.1207E-04	762.3628	22.8551	(A)	A (0.00)	A
164- 164	0.1216E-04	765.2610	22.9419	(A)	A (0.00)	A
165- 165	0.1222E-04	767.2849	23.0026	(A)	A (0.00)	A
166- 166	0.1246E-04	774.8018	23.2280	(A)	A (0.00)	A
167- 167	0.1256E-04	777.7901	23.3176	(A)	A (0.00)	A
168- 168	0.1264E-04	780.2822	23.3923	(A)	A (0.00)	A
169- 169	0.1274E-04	783.3682	23.4848	(A)	A (0.00)	A
170- 170	0.1289E-04	788.0585	23.6254	(A)	A (0.00)	A
171- 171	0.1293E-04	789.2817	23.6621	(A)	A (0.00)	A
172- 172	0.1303E-04	792.1401	23.7478	(A)	A (0.00)	A
173- 173	0.1325E-04	798.8435	23.9487	(A)	A (0.00)	A
174- 174	0.1338E-04	802.8024	24.0674	(A)	A (0.00)	A
175- 175	0.1347E-04	805.4111	24.1456	(A)	A (0.00)	A
176- 176	0.1367E-04	811.3475	24.3236	(A)	A (0.00)	A
177- 177	0.1679E-04	899.3327	26.9613	(A)	A (0.00)	A
178- 178	0.1830E-04	938.7684	28.1436	(A)	A (0.00)	A
179- 179	0.1936E-04	965.6564	28.9496	(A)	A (0.00)	A
180- 180	0.2152E-04	1018.2520	30.5259	(A)	A (0.00)	A
181- 181	0.2325E-04	1058.2355	31.7256	(A)	A (0.00)	A
182- 182	0.2337E-04	1060.9772	31.8073	(A)	A (0.00)	A
183- 183	0.2500E-04	1097.2730	32.8954	(A)	A (0.00)	A
184- 184	0.2541E-04	1106.2486	33.1645	(A)	A (0.00)	A
185- 185	0.2552E-04	1108.7462	33.2394	(A)	A (0.00)	A
186- 186	0.2566E-04	1111.7516	33.2995	(A)	A (0.00)	A
187- 187	0.2587E-04	1116.2654	33.4648	(A)	A (0.00)	A
188- 188	0.2610E-04	1120.8820	33.5732	(A)	A (0.00)	A
189- 189	0.2614E-04	1122.1760	33.6100	(A)	A (0.00)	A
190- 190	0.2630E-04	1125.8686	33.7411	(A)	A (0.00)	A
191- 191	0.2642E-04	1128.1371	33.8207	(A)	A (0.00)	A
192- 192	0.2671E-04	1134.2585	34.0042	(A)	A (0.00)	A
193- 193	0.2833E-04	1136.9008	34.0934	(A)	A (0.00)	A
194- 194	0.2694E-04	1139.0763	34.1486	(A)	A (0.00)	A
195- 195	0.2703E-04	1141.1010	34.2093	(A)	A (0.00)	A
196- 196	0.2724E-04	1145.5328	34.3422	(A)	A (0.00)	A
197- 197	0.2727E-04	1146.1428	34.3605	(A)	A (0.00)	A
198- 198	0.2747E-04	1150.2197	34.4827	(A)	A (0.00)	A
199- 199	0.2759E-04	1152.8566	34.5618	(A)	A (0.00)	A
200- 200	0.2766E-04	1154.2068	34.6022	(A)	A (0.00)	A
201- 201	0.2774E-04	1155.0667	34.6562	(A)	A (0.00)	A
202- 202	0.2793E-04	1159.8198	34.7705	(A)	A (0.00)	A
203- 203	0.2804E-04	1162.0878	34.8385	(A)	A (0.00)	A
204- 204	0.2811E-04	1163.6607	34.8857	(A)	A (0.00)	A
205- 205	0.2851E-04	1171.9421	35.1339	(A)	A (0.00)	A
206- 206	0.2856E-04	1172.8977	35.1626	(A)	A (0.00)	A

207- 207	0.2880E-04	1177.8628	35.3114	(A)	A (0.00)	A
208- 208	0.2885E-04	1178.7777	35.3389	(A)	A (0.00)	A
209- 209	0.2891E-04	1180.1167	35.3790	(A)	A (0.00)	A
210- 210	0.2899E-04	1181.6914	35.4262	(A)	A (0.00)	A
211- 211	0.2918E-04	1185.6612	35.5452	(A)	A (0.00)	A
212- 212	0.2926E-04	1187.2084	35.5916	(A)	A (0.00)	A
213- 213	0.2971E-04	1196.2821	35.8636	(A)	A (0.00)	A
214- 214	0.3042E-04	1210.4676	36.2889	(A)	A (0.00)	A
215- 215	0.3118E-04	1225.5455	36.7409	(A)	A (0.00)	A
216- 216	0.3184E-04	1238.4415	37.1275	(A)	A (0.00)	A
217- 217	0.3189E-04	1239.3097	37.1536	(A)	A (0.00)	A
218- 218	0.3250E-04	1251.1210	37.5077	(A)	A (0.00)	A
219- 219	0.3253E-04	1251.8235	37.5287	(A)	A (0.00)	A
220- 220	0.3301E-04	1261.0386	37.8050	(A)	A (0.00)	A
221- 221	0.3339E-04	1268.1038	38.0168	(A)	A (0.00)	A
222- 222	0.3369E-04	1273.6535	38.1832	(A)	A (0.00)	A
223- 223	0.3383E-04	1276.6045	38.2716	(A)	A (0.00)	A
224- 224	0.3391E-04	1278.0900	38.3162	(A)	A (0.00)	A
225- 225	0.3449E-04	1288.9224	38.6409	(A)	A (0.00)	A
226- 226	0.3588E-04	1314.6472	39.4121	(A)	A (0.00)	A
227- 227	0.5167E-04	1577.6966	47.2982	(A)	A (0.00)	A
228- 228	0.5303E-04	1598.2495	47.9143	(A)	A (0.00)	A
229- 229	0.2516E-03	3481.1061	104.3609	(A)	A (0.00)	A
230- 230	0.2636E-03	3563.6262	106.8348	(A)	A (0.00)	A
231- 231	0.2654E-03	3575.6994	107.1968	(A)	A (0.00)	A

Monometallic oxygen addition step

MODES		E (HARTREE**2)	FREQUENCIES		IRREP	IR	INTENS (KM/MOL)	RAMAN
			(CM**1)	(THZ)				
1- 1		-0.1097E-05	-229.8879	-6.8919	(A)	A (0.00)	A
2- 2		0.6256E-16	0.0000	0.0000	(A)	A (0.00)	A
3- 3		0.8059E-16	0.0000	0.0000	(A)	A (0.00)	A
4- 4		0.8496E-16	0.0000	0.0000	(A)	A (0.00)	A
5- 5		0.2477E-07	34.5390	1.0355	(A)	A (0.00)	A
6- 6		0.5755E-07	52.6527	1.5785	(A)	A (0.00)	A
7- 7		0.6387E-07	55.4673	1.6629	(A)	A (0.00)	A
8- 8		0.1087E-06	72.3822	2.1694	(A)	A (0.00)	A
9- 9		0.1138E-06	74.0282	2.2193	(A)	A (0.00)	A
10- 10		0.1369E-06	81.2121	2.4347	(A)	A (0.00)	A
11- 11		0.1679E-06	89.9422	2.6964	(A)	A (0.00)	A
12- 12		0.1823E-06	93.7070	2.8093	(A)	A (0.00)	A
13- 13		0.2012E-06	98.4492	2.9514	(A)	A (0.00)	A
14- 14		0.2212E-06	103.2235	3.0946	(A)	A (0.00)	A
15- 15		0.2695E-06	113.9313	3.4156	(A)	A (0.00)	A
16- 16		0.2739E-06	114.8552	3.4433	(A)	A (0.00)	A
17- 17		0.2970E-06	119.6171	3.5860	(A)	A (0.00)	A
18- 18		0.3056E-06	121.3345	3.6375	(A)	A (0.00)	A
19- 19		0.3200E-06	124.1513	3.7220	(A)	A (0.00)	A
20- 20		0.3279E-06	125.6752	3.7676	(A)	A (0.00)	A
21- 21		0.3578E-06	131.2905	3.9360	(A)	A (0.00)	A
22- 22		0.3631E-06	132.2447	3.9646	(A)	A (0.00)	A
23- 23		0.4082E-06	140.1653	4.2020	(A)	A (0.00)	A
24- 24		0.4333E-06	144.4744	4.3312	(A)	A (0.00)	A
25- 25		0.4365E-06	144.9957	4.3469	(A)	A (0.00)	A
26- 26		0.4641E-06	149.5136	4.4823	(A)	A (0.00)	A
27- 27		0.4956E-06	154.5106	4.6321	(A)	A (0.00)	A
28- 28		0.5067E-06	156.2296	4.6836	(A)	A (0.00)	A
29- 29		0.5196E-06	158.2108	4.7430	(A)	A (0.00)	A
30- 30		0.5400E-06	161.2831	4.8351	(A)	A (0.00)	A
31- 31		0.5596E-06	164.1877	4.9222	(A)	A (0.00)	A
32- 32		0.6082E-06	171.1600	5.1312	(A)	A (0.00)	A
33- 33		0.6282E-06	173.9568	5.2151	(A)	A (0.00)	A
34- 34		0.6482E-06	176.7064	5.2975	(A)	A (0.00)	A
35- 35		0.6555E-06	177.6915	5.3271	(A)	A (0.00)	A
36- 36		0.6767E-06	180.5438	5.4126	(A)	A (0.00)	A
37- 37		0.6971E-06	183.2399	5.4934	(A)	A (0.00)	A
38- 38		0.7087E-06	184.7633	5.5391	(A)	A (0.00)	A
39- 39		0.7322E-06	187.8073	5.6303	(A)	A (0.00)	A
40- 40		0.7569E-06	190.9464	5.7244	(A)	A (0.00)	A
41- 41		0.7754E-06	193.2655	5.7940	(A)	A (0.00)	A
42- 42		0.8240E-06	199.2247	5.9726	(A)	A (0.00)	A
43- 43		0.8515E-06	202.5011	6.0708	(A)	A (0.00)	A
44- 44		0.8699E-06	204.6668	6.1358	(A)	A (0.00)	A
45- 45		0.8755E-06	205.3560	6.1564	(A)	A (0.00)	A
46- 46		0.9257E-06	211.1591	6.3304	(A)	A (0.00)	A
47- 47		0.9402E-06	212.8152	6.3800	(A)	A (0.00)	A
48- 48		0.9617E-06	215.2351	6.4526	(A)	A (0.00)	A
49- 49		0.9804E-06	217.3132	6.5149	(A)	A (0.00)	A
50- 50		0.1007E-05	220.1907	6.6012	(A)	A (0.00)	A
51- 51		0.1028E-05	222.5231	6.6711	(A)	A (0.00)	A
52- 52		0.1094E-05	229.5274	6.8811	(A)	A (0.00)	A
53- 53		0.1132E-05	233.5120	7.0005	(A)	A (0.00)	A
54- 54		0.1164E-05	236.7928	7.0989	(A)	A (0.00)	A
55- 55		0.1182E-05	238.5978	7.1530	(A)	A (0.00)	A
56- 56		0.1196E-05	240.0142	7.1954	(A)	A (0.00)	A
57- 57		0.1250E-05	245.3560	7.3556	(A)	A (0.00)	A
58- 58		0.1293E-05	249.5173	7.4803	(A)	A (0.00)	A
59- 59		0.1324E-05	252.5113	7.5701	(A)	A (0.00)	A
60- 60		0.1354E-05	255.3736	7.6559	(A)	A (0.00)	A
61- 61		0.1439E-05	263.2866	7.8931	(A)	A (0.00)	A
62- 62		0.1466E-05	265.7666	7.9675	(A)	A (0.00)	A
63- 63		0.1475E-05	266.5923	7.9922	(A)	A (0.00)	A
64- 64		0.1515E-05	270.1076	8.0976	(A)	A (0.00)	A
65- 65		0.1551E-05	273.2982	8.1933	(A)	A (0.00)	A
66- 66		0.1595E-05	277.1835	8.3098	(A)	A (0.00)	A
67- 67		0.1634E-05	280.5328	8.4102	(A)	A (0.00)	A
68- 68		0.1669E-05	283.5016	8.4992	(A)	A (0.00)	A
69- 69		0.1725E-05	288.2850	8.6426	(A)	A (0.00)	A
70- 70		0.1758E-05	291.0003	8.7240	(A)	A (0.00)	A
71- 71		0.1804E-05	294.8038	8.8380	(A)	A (0.00)	A
72- 72		0.1863E-05	299.5440	8.9801	(A)	A (0.00)	A
73- 73		0.1909E-05	303.2172	9.0902	(A)	A (0.00)	A
74- 74		0.1958E-05	307.1024	9.2067	(A)	A (0.00)	A
75- 75		0.2080E-05	316.4966	9.4883	(A)	A (0.00)	A
76- 76		0.2153E-05	322.0307	9.6542	(A)	A (0.00)	A
77- 77		0.2259E-05	329.8669	9.8892	(A)	A (0.00)	A
78- 78		0.2392E-05	339.4219	10.1756	(A)	A (0.00)	A
79- 79		0.2538E-05	349.6160	10.4812	(A)	A (0.00)	A
80- 80		0.2608E-05	354.4317	10.6256	(A)	A (0.00)	A
81- 81		0.2705E-05	360.9862	10.8221	(A)	A (0.00)	A

82- 82	0.2725E-05	362.2984	10.8614	(A)	A (0.00)	A
83- 83	0.2932E-05	375.8137	11.2666	(A)	A (0.00)	A
84- 84	0.2993E-05	379.6700	11.3822	(A)	A (0.00)	A
85- 85	0.3012E-05	380.9282	11.4199	(A)	A (0.00)	A
86- 86	0.3072E-05	384.6608	11.5318	(A)	A (0.00)	A
87- 87	0.3150E-05	389.5358	11.6780	(A)	A (0.00)	A
88- 88	0.3168E-05	390.6555	11.7116	(A)	A (0.00)	A
89- 89	0.3200E-05	392.6258	11.7706	(A)	A (0.00)	A
90- 90	0.3228E-05	394.3248	11.8216	(A)	A (0.00)	A
91- 91	0.3243E-05	395.2635	11.8497	(A)	A (0.00)	A
92- 92	0.3386E-05	403.8653	12.1076	(A)	A (0.00)	A
93- 93	0.3465E-05	408.5557	12.2482	(A)	A (0.00)	A
94- 94	0.3497E-05	410.4154	12.3039	(A)	A (0.00)	A
95- 95	0.3588E-05	415.7570	12.4641	(A)	A (0.00)	A
96- 96	0.3623E-05	417.7561	12.5240	(A)	A (0.00)	A
97- 97	0.3676E-05	420.8170	12.6158	(A)	A (0.00)	A
98- 98	0.3703E-05	422.3467	12.6616	(A)	A (0.00)	A
99- 99	0.3744E-05	424.6588	12.7309	(A)	A (0.00)	A
100- 100	0.3770E-05	426.1204	12.7748	(A)	A (0.00)	A
101- 101	0.3846E-05	430.4197	12.9037	(A)	A (0.00)	A
102- 102	0.3876E-05	432.1071	12.9542	(A)	A (0.00)	A
103- 103	0.3943E-05	435.8281	13.0658	(A)	A (0.00)	A
104- 104	0.3989E-05	438.3322	13.1409	(A)	A (0.00)	A
105- 105	0.4105E-05	444.6486	13.3302	(A)	A (0.00)	A
106- 106	0.4148E-05	447.0112	13.4011	(A)	A (0.00)	A
107- 107	0.4289E-05	454.5124	13.6259	(A)	A (0.00)	A
108- 108	0.4333E-05	456.8438	13.6958	(A)	A (0.00)	A
109- 109	0.4382E-05	459.4423	13.7737	(A)	A (0.00)	A
110- 110	0.4393E-05	459.9975	13.7904	(A)	A (0.00)	A
111- 111	0.4415E-05	461.1521	13.8250	(A)	A (0.00)	A
112- 112	0.4521E-05	466.6641	13.9902	(A)	A (0.00)	A
113- 113	0.4605E-05	470.9714	14.1194	(A)	A (0.00)	A
114- 114	0.4653E-05	473.4442	14.1935	(A)	A (0.00)	A
115- 115	0.4723E-05	476.9842	14.2996	(A)	A (0.00)	A
116- 116	0.4751E-05	478.4007	14.3421	(A)	A (0.00)	A
117- 117	0.4872E-05	484.4311	14.5229	(A)	A (0.00)	A
118- 118	0.4930E-05	487.2977	14.6088	(A)	A (0.00)	A
119- 119	0.4960E-05	488.7780	14.6532	(A)	A (0.00)	A
120- 120	0.5013E-05	491.3889	14.7315	(A)	A (0.00)	A
121- 121	0.5026E-05	492.0322	14.7508	(A)	A (0.00)	A
122- 122	0.5106E-05	495.9243	14.8674	(A)	A (0.00)	A
123- 123	0.5155E-05	498.3175	14.9392	(A)	A (0.00)	A
124- 124	0.5239E-05	502.3720	15.0607	(A)	A (0.00)	A
125- 125	0.5323E-05	506.3746	15.1807	(A)	A (0.00)	A
126- 126	0.5420E-05	510.9787	15.3188	(A)	A (0.00)	A
127- 127	0.5553E-05	517.1820	15.5047	(A)	A (0.00)	A
128- 128	0.5683E-05	518.5585	15.5468	(A)	A (0.00)	A
129- 129	0.5675E-05	522.8175	15.6737	(A)	A (0.00)	A
130- 130	0.5776E-05	527.4893	15.8131	(A)	A (0.00)	A
131- 131	0.5914E-05	533.7211	16.0006	(A)	A (0.00)	A
132- 132	0.5998E-05	537.5131	16.1142	(A)	A (0.00)	A
133- 133	0.6181E-05	545.6361	16.3578	(A)	A (0.00)	A
134- 134	0.6331E-05	552.2627	16.5553	(A)	A (0.00)	A
135- 135	0.6461E-05	557.8535	16.7240	(A)	A (0.00)	A
136- 136	0.6697E-05	567.9545	17.0268	(A)	A (0.00)	A
137- 137	0.6722E-05	569.0171	17.0587	(A)	A (0.00)	A
138- 138	0.6892E-05	576.1625	17.2729	(A)	A (0.00)	A
139- 139	0.6892E-05	579.9202	17.3856	(A)	A (0.00)	A
140- 140	0.7117E-05	585.5057	17.5530	(A)	A (0.00)	A
141- 141	0.7243E-05	590.6647	17.7077	(A)	A (0.00)	A
142- 142	0.7960E-05	619.2289	18.5640	(A)	A (0.00)	A
143- 143	0.8011E-05	639.9262	19.1845	(A)	A (0.00)	A
144- 144	0.8626E-05	644.6013	19.3247	(A)	A (0.00)	A
145- 145	0.8973E-05	657.4329	19.7093	(A)	A (0.00)	A
146- 146	0.9133E-05	663.2851	19.8848	(A)	A (0.00)	A
147- 147	0.9203E-05	665.8107	19.9605	(A)	A (0.00)	A
148- 148	0.9433E-05	667.2624	20.0040	(A)	A (0.00)	A
149- 149	0.9650E-05	681.7789	20.4392	(A)	A (0.00)	A
150- 150	0.9755E-05	684.6322	20.5086	(A)	A (0.00)	A
151- 151	0.9871E-05	689.6635	20.5878	(A)	A (0.00)	A
152- 152	0.1033E-04	705.5299	21.1513	(A)	A (0.00)	A
153- 153	0.1071E-04	718.2285	21.5319	(A)	A (0.00)	A
154- 154	0.1106E-04	730.0204	21.8855	(A)	A (0.00)	A
155- 155	0.1117E-04	733.5090	21.9900	(A)	A (0.00)	A
156- 156	0.1124E-04	735.6894	22.0554	(A)	A (0.00)	A
157- 157	0.1145E-04	742.6319	22.2635	(A)	A (0.00)	A
158- 158	0.1155E-04	746.0478	22.3660	(A)	A (0.00)	A
159- 159	0.1182E-04	754.3995	22.6163	(A)	A (0.00)	A
160- 160	0.1190E-04	757.1358	22.6984	(A)	A (0.00)	A
161- 161	0.1195E-04	758.5807	22.7417	(A)	A (0.00)	A
162- 162	0.1214E-04	764.6297	22.9231	(A)	A (0.00)	A
163- 163	0.1222E-04	767.3009	23.0030	(A)	A (0.00)	A
164- 164	0.1225E-04	768.0361	23.0251	(A)	A (0.00)	A
165- 165	0.1231E-04	769.9649	23.0805	(A)	A (0.00)	A
166- 166	0.1246E-04	774.3793	23.2261	(A)	A (0.00)	A
167- 167	0.1254E-04	777.0469	23.2953	(A)	A (0.00)	A
168- 168	0.1265E-04	780.7221	23.4055	(A)	A (0.00)	A
169- 169	0.1272E-04	782.7293	23.4656	(A)	A (0.00)	A
170- 170	0.1296E-04	790.1920	23.6894	(A)	A (0.00)	A
171- 171	0.1303E-04	792.1452	23.7479	(A)	A (0.00)	A
172- 172	0.1315E-04	795.9460	23.8619	(A)	A (0.00)	A
173- 173	0.1319E-04	797.0122	23.8938	(A)	A (0.00)	A
174- 174	0.1327E-04	799.3608	23.9642	(A)	A (0.00)	A
175- 175	0.1364E-04	810.5021	24.2982	(A)	A (0.00)	A
176- 176	0.1373E-04	813.1901	24.3788	(A)	A (0.00)	A
177- 177	0.1404E-04	822.4322	24.6556	(A)	A (0.00)	A
178- 178	0.1488E-04	917.6030	27.5099	(A)	A (0.00)	A
179- 179	0.1911E-04	959.3772	28.7614	(A)	A (0.00)	A
180- 180	0.2140E-04	1016.1950	30.4643	(A)	A (0.00)	A
181- 181	0.2494E-04	1095.2026	32.8838	(A)	A (0.00)	A
182- 182	0.2502E-04	1097.8905	32.9139	(A)	A (0.00)	A
183- 183	0.2587E-04	1111.9329	33.3349	(A)	A (0.00)	A
184- 184	0.2572E-04	1113.1627	33.3718	(A)	A (0.00)	A
185- 185	0.2995E-04	1117.9982	33.5167	(A)	A (0.00)	A
186- 186	0.2613E-04	1121.8597	33.6324	(A)	A (0.00)	A
187- 187	0.2672E-04	1127.3573	33.7871	(A)	A (0.00)	A
188- 188	0.2652E-04	1130.1452	33.8999	(A)	A (0.00)	A
189- 189	0.2655E-04	1130.9276	33.9044	(A)	A (0.00)	A
190- 190	0.2667E-04	1132.3285	33.9763	(A)	A (0.00)	A
191- 191	0.2671E-04	1134.3646	34.0069	(A)	A (0.00)	A
192- 192	0.2679E-04	1136.0364	34.0575	(A)	A (0.00)	A
193- 193	0.2682E-04	1136.7085	34.0777	(A)	A (0.00)	A
194- 194	0.2685E-04	1137.1527	34.0910	(A)	A (0.00)	A
195- 195	0.2698E-04	1139.9928	34.1761	(A)	A (0.00)	A
196- 196	0.2703E-04	1140.9602	34.2051	(A)	A (0.00)	A
197- 197	0.2717E-04	1143.9233	34.2940	(A)	A (0.00)	A
198- 198	0.2724E-04	1145.4986	34.3412	(A)	A (0.00)	A
199- 199	0.2735E-04	1147.7566	34.4089	(A)	A (0.00)	A
200- 200	0.2739E-04	1148.5554	34.4329	(A)	A (0.00)	A

201-	201	0.2749E-04	1150.7221	34.4978	(A)	A (0.00)	A
202-	202	0.2752E-04	1151.3347	34.5161	(A)	A (0.00)	A
203-	203	0.2773E-04	1155.7153	34.6475	(A)	A (0.00)	A
204-	204	0.2775E-04	1156.2115	34.6623	(A)	A (0.00)	A
205-	205	0.2799E-04	1161.2093	34.8122	(A)	A (0.00)	A
206-	206	0.2805E-04	1162.2858	34.8445	(A)	A (0.00)	A
207-	207	0.2808E-04	1163.0723	34.8680	(A)	A (0.00)	A
208-	208	0.2826E-04	1166.8079	34.9800	(A)	A (0.00)	A
209-	209	0.2831E-04	1167.8176	35.0103	(A)	A (0.00)	A
210-	210	0.2845E-04	1170.6148	35.0941	(A)	A (0.00)	A
211-	211	0.2847E-04	1171.0242	35.1064	(A)	A (0.00)	A
212-	212	0.2865E-04	1174.6730	35.2158	(A)	A (0.00)	A
213-	213	0.2893E-04	1180.3938	35.3873	(A)	A (0.00)	A
214-	214	0.2917E-04	1185.4670	35.5394	(A)	A (0.00)	A
215-	215	0.2926E-04	1187.1537	35.5900	(A)	A (0.00)	A
216-	216	0.3030E-04	1208.1783	36.2203	(A)	A (0.00)	A
217-	217	0.3082E-04	1218.3595	36.5255	(A)	A (0.00)	A
218-	218	0.3187E-04	1239.0714	37.1464	(A)	A (0.00)	A
219-	219	0.3231E-04	1247.6139	37.4025	(A)	A (0.00)	A
220-	220	0.3265E-04	1254.0028	37.5941	(A)	A (0.00)	A
221-	221	0.3281E-04	1257.1799	37.6893	(A)	A (0.00)	A
222-	222	0.3297E-04	1260.2408	37.7811	(A)	A (0.00)	A
223-	223	0.3332E-04	1266.8853	37.9803	(A)	A (0.00)	A
224-	224	0.3335E-04	1267.4535	37.9973	(A)	A (0.00)	A
225-	225	0.3360E-04	1272.1440	38.1379	(A)	A (0.00)	A
226-	226	0.3382E-04	1276.3044	38.2626	(A)	A (0.00)	A
227-	227	0.3401E-04	1280.0054	38.3736	(A)	A (0.00)	A
228-	228	0.3459E-04	1290.7510	38.6957	(A)	A (0.00)	A
229-	229	0.4145E-04	1412.9474	42.3591	(A)	A (0.00)	A
230-	230	0.4787E-04	1518.4887	45.5231	(A)	A (0.00)	A
231-	231	0.4937E-04	1542.1849	46.2335	(A)	A (0.00)	A
232-	232	0.9418E-04	2129.9440	63.8541	(A)	A (0.00)	A
233-	233	0.2292E-03	3322.8688	99.6171	(A)	A (0.00)	A
234-	234	0.2557E-03	3509.4879	105.2118	(A)	A (0.00)	A

75-	75	0.1980E-05	308.9274	9.2584	(A)	A (0.00)	A
76-	76	0.2007E-05	310.9189	9.3211	(A)	A (0.00)	A
77-	77	0.2113E-05	318.9946	9.5632	(A)	A (0.00)	A
78-	78	0.2142E-05	321.2168	9.6298	(A)	A (0.00)	A
79-	79	0.2242E-05	328.6258	9.8520	(A)	A (0.00)	A
80-	80	0.2297E-05	332.6500	9.9726	(A)	A (0.00)	A
81-	81	0.2358E-05	337.0384	10.1042	(A)	A (0.00)	A
82-	82	0.2437E-05	342.5849	10.2704	(A)	A (0.00)	A
83-	83	0.2631E-05	356.0118	10.6730	(A)	A (0.00)	A
84-	84	0.2647E-05	357.0534	10.7042	(A)	A (0.00)	A
85-	85	0.2830E-05	369.1839	11.0679	(A)	A (0.00)	A
86-	86	0.2897E-05	373.5276	11.1981	(A)	A (0.00)	A
87-	87	0.2943E-05	376.5066	11.2874	(A)	A (0.00)	A
88-	88	0.3004E-05	380.3818	11.4036	(A)	A (0.00)	A
89-	89	0.3080E-05	385.1571	11.5467	(A)	A (0.00)	A
90-	90	0.3115E-05	387.3749	11.6132	(A)	A (0.00)	A
91-	91	0.3140E-05	388.9231	11.6596	(A)	A (0.00)	A
92-	92	0.3190E-05	391.9894	11.7515	(A)	A (0.00)	A
93-	93	0.3261E-05	396.3335	11.8818	(A)	A (0.00)	A
94-	94	0.3328E-05	400.4031	12.0038	(A)	A (0.00)	A
95-	95	0.3439E-05	407.0017	12.2016	(A)	A (0.00)	A
96-	96	0.3501E-05	410.6674	12.3115	(A)	A (0.00)	A
97-	97	0.3587E-05	415.6754	12.4616	(A)	A (0.00)	A
98-	98	0.3619E-05	417.5497	12.5178	(A)	A (0.00)	A
99-	99	0.3642E-05	418.8538	12.5569	(A)	A (0.00)	A
100-	100	0.3666E-05	420.2016	12.5973	(A)	A (0.00)	A
101-	101	0.3706E-05	422.4918	12.6660	(A)	A (0.00)	A
102-	102	0.3754E-05	425.2097	12.7475	(A)	A (0.00)	A
103-	103	0.3814E-05	428.6268	12.8499	(A)	A (0.00)	A
104-	104	0.3853E-05	430.7956	12.9149	(A)	A (0.00)	A
105-	105	0.3943E-05	435.8059	13.0651	(A)	A (0.00)	A
106-	106	0.3991E-05	438.4700	13.1450	(A)	A (0.00)	A
107-	107	0.4110E-05	444.9270	13.3386	(A)	A (0.00)	A
108-	108	0.4153E-05	447.2504	13.4082	(A)	A (0.00)	A
109-	109	0.4166E-05	447.9632	13.4296	(A)	A (0.00)	A
110-	110	0.4279E-05	453.9853	13.6101	(A)	A (0.00)	A
111-	111	0.4383E-05	459.4686	13.7745	(A)	A (0.00)	A
112-	112	0.4489E-05	465.0260	13.9411	(A)	A (0.00)	A
113-	113	0.4543E-05	467.8052	14.0244	(A)	A (0.00)	A
114-	114	0.4574E-05	469.3736	14.0715	(A)	A (0.00)	A
115-	115	0.4611E-05	471.2622	14.1281	(A)	A (0.00)	A
116-	116	0.4686E-05	475.0976	14.2431	(A)	A (0.00)	A
117-	117	0.4748E-05	478.2157	14.3365	(A)	A (0.00)	A
118-	118	0.4851E-05	483.4015	14.4920	(A)	A (0.00)	A
119-	119	0.4906E-05	486.1302	14.5738	(A)	A (0.00)	A
120-	120	0.4947E-05	488.1312	14.6338	(A)	A (0.00)	A
121-	121	0.4989E-05	489.2150	14.6663	(A)	A (0.00)	A
122-	122	0.5007E-05	491.1053	14.7230	(A)	A (0.00)	A
123-	123	0.5069E-05	494.1120	14.8131	(A)	A (0.00)	A
124-	124	0.5155E-05	498.3223	14.9393	(A)	A (0.00)	A
125-	125	0.5221E-05	501.4954	15.0345	(A)	A (0.00)	A
126-	126	0.5338E-05	507.0635	15.2014	(A)	A (0.00)	A
127-	127	0.5470E-05	513.3178	15.3889	(A)	A (0.00)	A
128-	128	0.5532E-05	516.2201	15.4759	(A)	A (0.00)	A
129-	129	0.5661E-05	522.1726	15.6543	(A)	A (0.00)	A
130-	130	0.5850E-05	530.8384	15.9141	(A)	A (0.00)	A
131-	131	0.5981E-05	536.7424	16.0911	(A)	A (0.00)	A
132-	132	0.6115E-05	542.7170	16.2702	(A)	A (0.00)	A
133-	133	0.6270E-05	549.5536	16.4752	(A)	A (0.00)	A
134-	134	0.6450E-05	557.3789	16.7098	(A)	A (0.00)	A
135-	135	0.6650E-05	565.9738	16.9675	(A)	A (0.00)	A
136-	136	0.6822E-05	567.3485	17.0087	(A)	A (0.00)	A
137-	137	0.6793E-05	572.0193	17.1487	(A)	A (0.00)	A
138-	138	0.6857E-05	574.7085	17.2293	(A)	A (0.00)	A
139-	139	0.7004E-05	580.8494	17.4134	(A)	A (0.00)	A
140-	140	0.7144E-05	586.6122	17.5862	(A)	A (0.00)	A
141-	141	0.7187E-05	588.3653	17.6387	(A)	A (0.00)	A
142-	142	0.7358E-05	595.3251	17.8474	(A)	A (0.00)	A
143-	143	0.8019E-05	621.4917	18.6319	(A)	A (0.00)	A
144-	144	0.8058E-05	623.0015	18.6771	(A)	A (0.00)	A
145-	145	0.8373E-05	635.0788	19.0392	(A)	A (0.00)	A
146-	146	0.8650E-05	645.5031	19.3517	(A)	A (0.00)	A
147-	147	0.8988E-05	657.9972	19.7263	(A)	A (0.00)	A
148-	148	0.9170E-05	664.6066	19.9244	(A)	A (0.00)	A
149-	149	0.9236E-05	667.0050	19.9963	(A)	A (0.00)	A
150-	150	0.9536E-05	677.7388	20.3181	(A)	A (0.00)	A
151-	151	0.9745E-05	685.1509	20.5403	(A)	A (0.00)	A
152-	152	0.1000E-04	694.1116	20.8089	(A)	A (0.00)	A
153-	153	0.1014E-04	698.8013	20.9495	(A)	A (0.00)	A
154-	154	0.1051E-04	711.6355	21.3343	(A)	A (0.00)	A
155-	155	0.1067E-04	716.7676	21.4882	(A)	A (0.00)	A
156-	156	0.1089E-04	724.1207	21.7086	(A)	A (0.00)	A
157-	157	0.1091E-04	724.8942	21.7318	(A)	A (0.00)	A
158-	158	0.1102E-04	728.7211	21.8465	(A)	A (0.00)	A
159-	159	0.1123E-04	735.3263	22.0445	(A)	A (0.00)	A
160-	160	0.1140E-04	741.0228	22.2153	(A)	A (0.00)	A
161-	161	0.1156E-04	746.3543	22.3751	(A)	A (0.00)	A
162-	162	0.1162E-04	748.2574	22.4322	(A)	A (0.00)	A
163-	163	0.1168E-04	750.1932	22.4902	(A)	A (0.00)	A
164-	164	0.1187E-04	756.2149	22.6708	(A)	A (0.00)	A
165-	165	0.1191E-04	757.4697	22.7084	(A)	A (0.00)	A
166-	166	0.1204E-04	761.4758	22.8285	(A)	A (0.00)	A
167-	167	0.1205E-04	761.9044	22.8413	(A)	A (0.00)	A
168-	168	0.1231E-04	770.1026	23.0871	(A)	A (0.00)	A
169-	169	0.1232E-04	770.3993	23.0960	(A)	A (0.00)	A
170-	170	0.1238E-04	772.0727	23.1462	(A)	A (0.00)	A
171-	171	0.1252E-04	776.6326	23.2829	(A)	A (0.00)	A
172-	172	0.1257E-04	778.2594	23.3316	(A)	A (0.00)	A
173-	173	0.1271E-04	782.4260	23.4565	(A)	A (0.00)	A
174-	174	0.1286E-04	787.0126	23.5940	(A)	A (0.00)	A
175-	175	0.1292E-04	788.9158	23.6511	(A)	A (0.00)	A
176-	176	0.1302E-04	791.9073	23.7408	(A)	A (0.00)	A
177-	177	0.1316E-04	796.1535	23.8681	(A)	A (0.00)	A
178-	178	0.1333E-04	801.2522	24.0209	(A)	A (0.00)	A
179-	179	0.1345E-04	804.8549	24.1289	(A)	A (0.00)	A
180-	180	0.1368E-04	811.8610	24.3390	(A)	A (0.00)	A
181-	181	0.1745E-04	916.7451	27.4933	(A)	A (0.00)	A
182-	182	0.1876E-04	950.6939	28.5012	(A)	A (0.00)	A
183-	183	0.1955E-04	970.3013	29.0889	(A)	A (0.00)	A
184-	184	0.2258E-04	1042.9011	31.2624	(A)	A (0.00)	A
185-	185	0.2328E-04	1058.9617	31.7469	(A)	A (0.00)	A
186-	186	0.2392E-04	1073.3089	32.1770	(A)	A (0.00)	A
187-	187	0.2467E-04	1090.1070	32.6606	(A)	A (0.00)	A
188-	188	0.2483E-04	1093.6543	32.7875	(A)	A (0.00)	A
189-	189	0.2524E-04	1102.5717	33.0537	(A)	A (0.00)	A
190-	190	0.2545E-04	1107.1401	33.1912	(A)	A (0.00)	A
191-	191	0.2569E-04	1112.3681	33.3480	(A)	A (0.00)	A
192-	192	0.2582E-04	1115.1443	33.4312	(A)	A (0.00)	A
193-	193	0.2591E-04	1117.0626	33.4887	(A)	A (0.00)	A

194- 194	0.2616E-04	1122.5774	33.6540	(A)	A (0.00)	A
195- 195	0.2631E-04	1125.7401	33.7488	(A)	A (0.00)	A
196- 196	0.2647E-04	1129.1015	33.8496	(A)	A (0.00)	A
197- 197	0.2655E-04	1130.9515	33.9051	(A)	A (0.00)	A
198- 198	0.2665E-04	1133.0041	33.9666	(A)	A (0.00)	A
199- 199	0.2678E-04	1135.8230	34.0511	(A)	A (0.00)	A
200- 200	0.2689E-04	1138.1383	34.1205	(A)	A (0.00)	A
201- 201	0.2698E-04	1140.0039	34.1765	(A)	A (0.00)	A
202- 202	0.2712E-04	1143.0591	34.2680	(A)	A (0.00)	A
203- 203	0.2725E-04	1145.6750	34.3465	(A)	A (0.00)	A
204- 204	0.2743E-04	1149.5039	34.4613	(A)	A (0.00)	A
205- 205	0.2758E-04	1152.6179	34.5546	(A)	A (0.00)	A
206- 206	0.2782E-04	1157.7153	34.7074	(A)	A (0.00)	A
207- 207	0.2787E-04	1158.6872	34.7366	(A)	A (0.00)	A
208- 208	0.2794E-04	1160.1868	34.7815	(A)	A (0.00)	A
209- 209	0.2806E-04	1162.6350	34.8549	(A)	A (0.00)	A
210- 210	0.2824E-04	1166.3220	34.9655	(A)	A (0.00)	A
211- 211	0.2829E-04	1167.3274	34.9956	(A)	A (0.00)	A
212- 212	0.2847E-04	1171.1156	35.1092	(A)	A (0.00)	A
213- 213	0.2856E-04	1172.8394	35.1608	(A)	A (0.00)	A
214- 214	0.2885E-04	1178.8789	35.3419	(A)	A (0.00)	A
215- 215	0.2886E-04	1179.0546	35.3472	(A)	A (0.00)	A
216- 216	0.2892E-04	1180.2213	35.3821	(A)	A (0.00)	A
217- 217	0.2923E-04	1186.6513	35.5749	(A)	A (0.00)	A
218- 218	0.2954E-04	1192.9400	35.7634	(A)	A (0.00)	A
219- 219	0.2956E-04	1193.1779	35.7706	(A)	A (0.00)	A
220- 220	0.3054E-04	1212.8515	36.3604	(A)	A (0.00)	A
221- 221	0.3180E-04	1237.7286	37.1062	(A)	A (0.00)	A
222- 222	0.3196E-04	1240.7514	37.1968	(A)	A (0.00)	A
223- 223	0.3208E-04	1243.0382	37.2653	(A)	A (0.00)	A
224- 224	0.3272E-04	1255.3372	37.6341	(A)	A (0.00)	A
225- 225	0.3275E-04	1256.0770	37.6562	(A)	A (0.00)	A
226- 226	0.3331E-04	1266.6325	37.9727	(A)	A (0.00)	A
227- 227	0.3360E-04	1272.2175	38.1401	(A)	A (0.00)	A
228- 228	0.3388E-04	1277.4900	38.2982	(A)	A (0.00)	A
229- 229	0.3424E-04	1284.3380	38.5035	(A)	A (0.00)	A
230- 230	0.3458E-04	1290.6902	38.6939	(A)	A (0.00)	A
231- 231	0.4332E-04	1444.4853	43.3046	(A)	A (0.00)	A
232- 232	0.5193E-04	1581.6154	47.4156	(A)	A (0.00)	A
233- 233	0.2491E-03	3463.8488	103.8436	(A)	A (0.00)	A
234- 234	0.2628E-03	3557.6053	106.6543	(A)	A (0.00)	A
235- 235	0.2639E-03	3565.0860	106.8786	(A)	A (0.00)	A
236- 236	0.3138E-03	3888.0400	116.5605	(A)	A (0.00)	A

Transition state figures

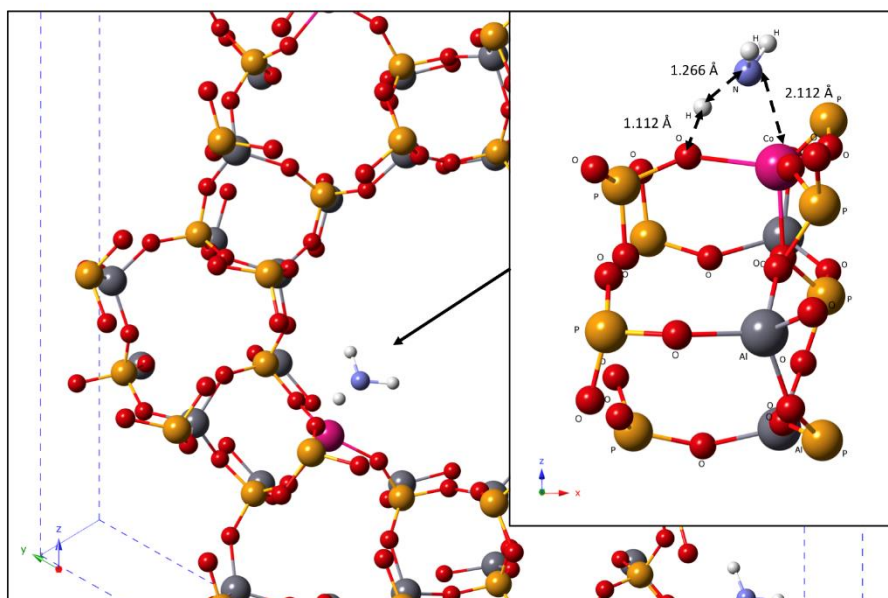


Figure S12: The calculated transition state for the monometallic CoAlPO-5 system during the hydrogen abstraction step. Pink = Cobalt, Red = Oxygen, Yellow = Phosphorus, Grey = Aluminium, White = Hydrogen, Blue = Nitrogen.

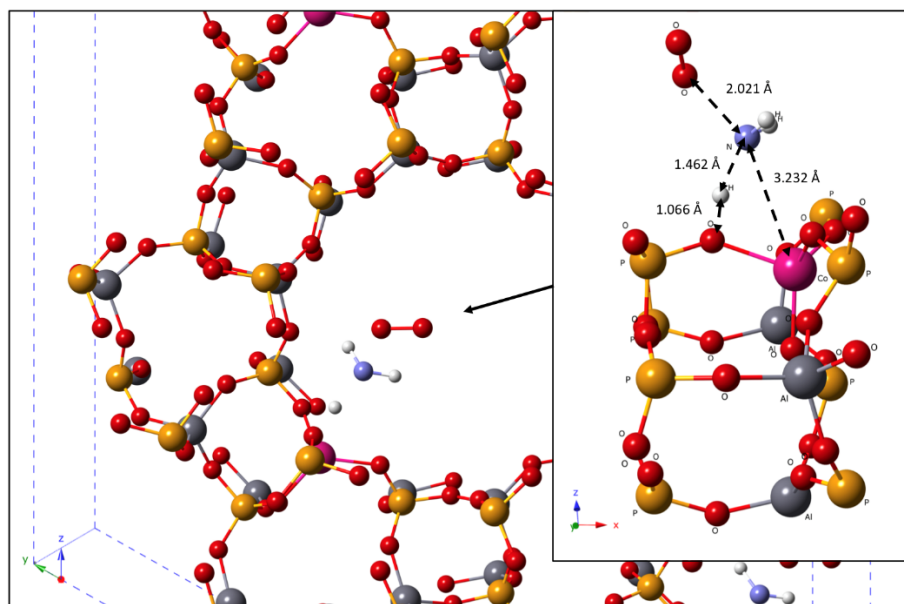


Figure S13: The calculated transition state for the monometallic CoAlPO-5 system during the oxygen addition step. Pink = Cobalt, Red = Oxygen, Yellow = Phosphorus, Grey = Aluminium, White = Hydrogen, Blue = Nitrogen.

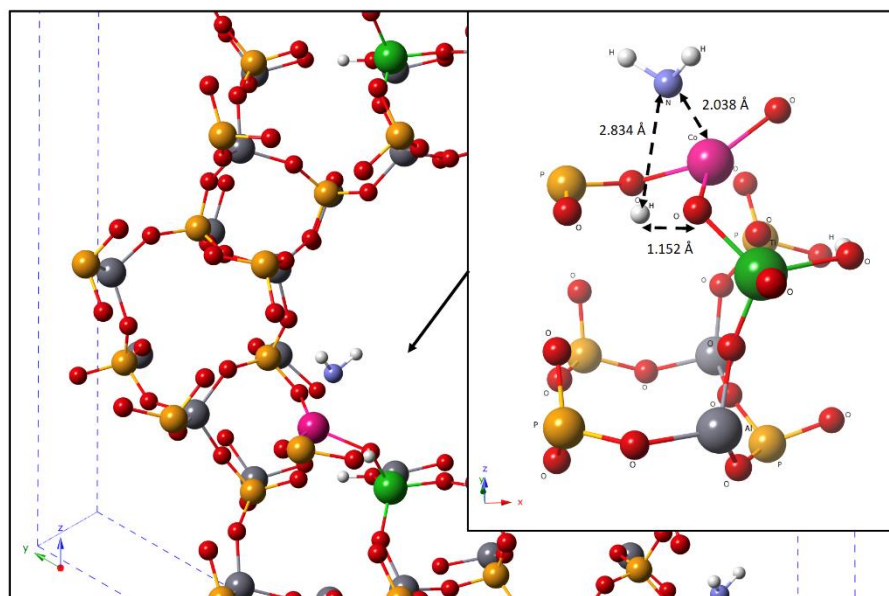


Figure S14: The calculated transition state for the bimetallic CoTiAlPO-5 system during the hydrogen abstraction step. Pink = Cobalt, Green = Titanium, Red = Oxygen, Yellow = Phosphorus, Grey = Aluminium, White = Hydrogen, Blue = Nitrogen.

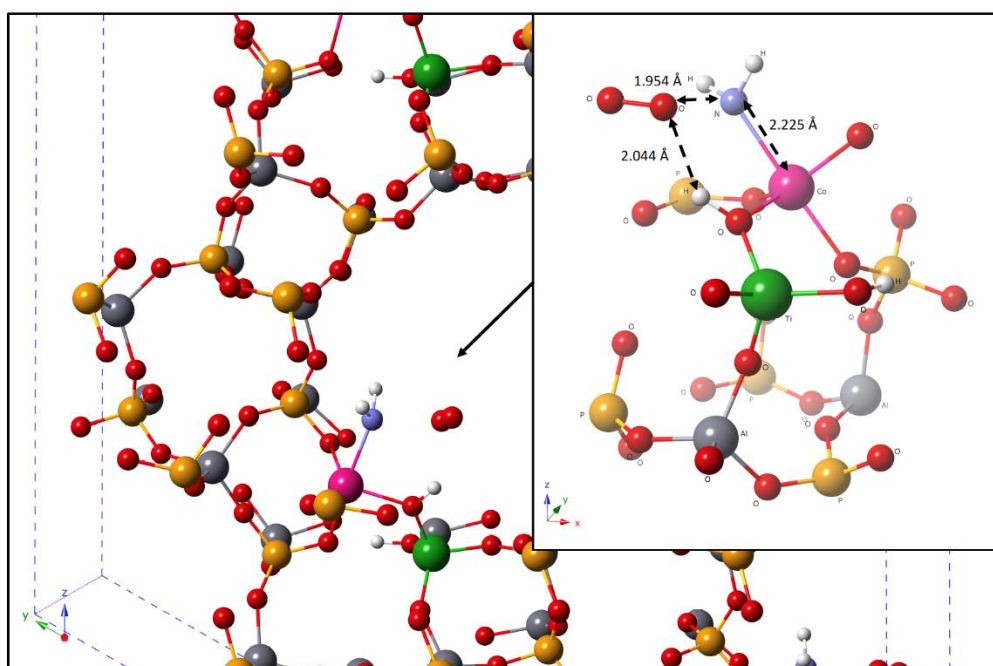


Figure S15: The calculated transition state for the bimetallic CoTiAlPO-5 system during the oxygen addition step. Pink = Cobalt, Green = Titanium, Red = Oxygen, Yellow = Phosphorus, Grey = Aluminium, White = Hydrogen, Blue = Nitrogen.

Complete reaction energetics

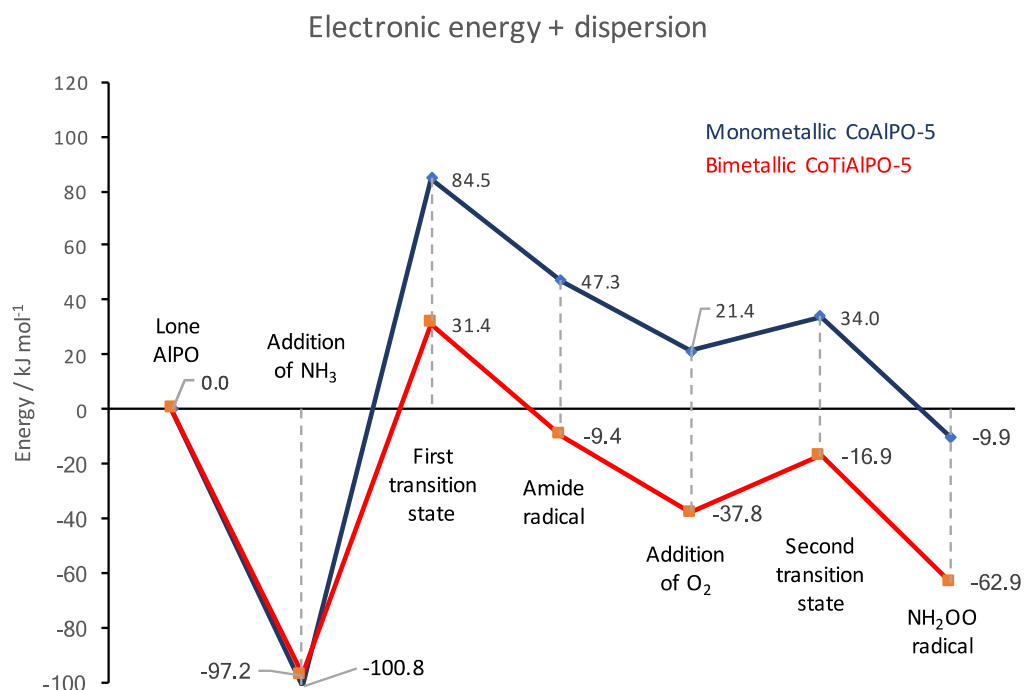


Figure S16: Full comparison of the complete electronic energetics required in the first two reaction steps, calculated with the addition of the dispersion correction.

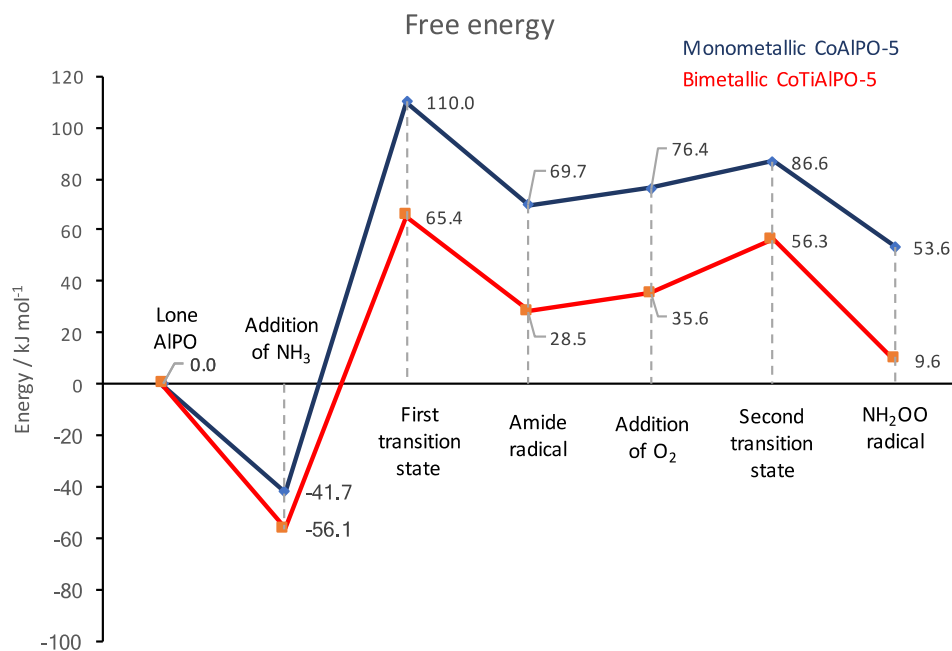


Figure S17: Full comparison of the complete free energy energetics required in the first two reaction steps, estimated by the addition of vibrational entropy and zero-point energy.

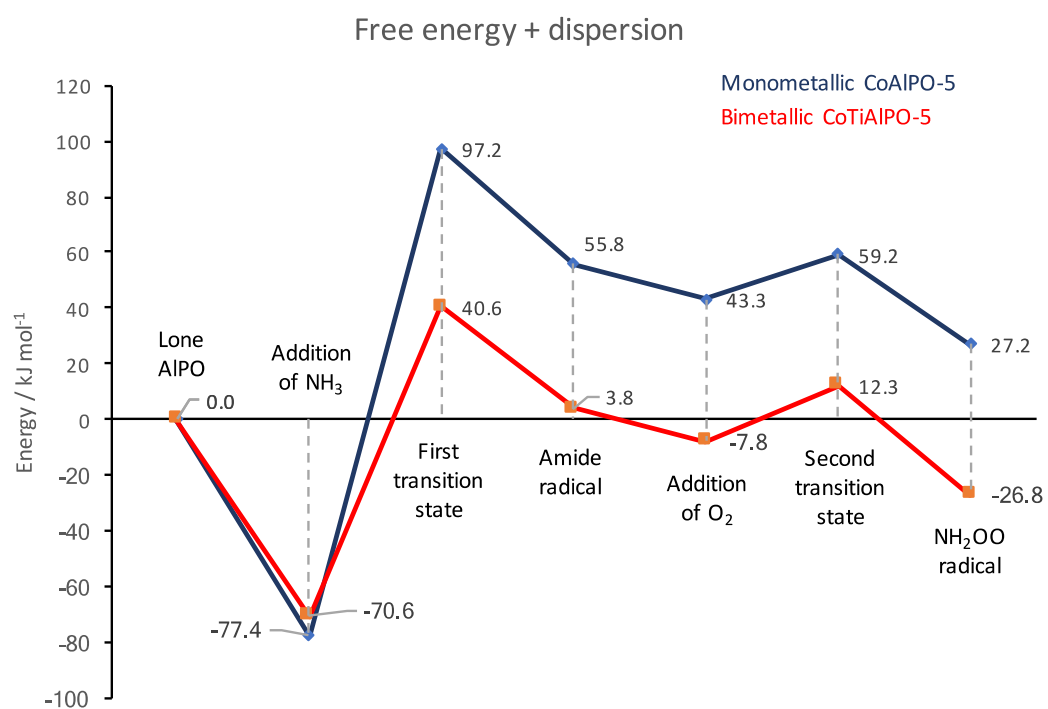


Figure S18: Full comparison of the complete free energy energetics required in the first two reaction steps, with the addition of the dispersion correction.